2018

The role of channel fens in permafrost degradation induced changes in peatland discharge at Scotty Creek, NT

Lindsay Elena Stone
Wilfrid Laurier University, ston5270@mylaurier.ca

The role of channel fens in permafrost degradation induced changes in peatland discharge at Scotty Creek, NT

By

Lindsay Elena Stone

BSc, McGill University, 2013

THESIS

Submitted to the Department of Geography and Environmental Studies

In partial fulfillment of the requirements for

Master of Science in Geography

Wilfrid Laurier University

AUTHOR'S DECLARATION

I hereby declare that I am the sole author of this thesis. This is a true copy of the thesis, including any required final revision, as accepted by my examiners.

I understand that my thesis may be electronically available to the public.

DECLARATION OF CO-AUTHORSHIP

This thesis is the result of collaborative work with the co-authors listed in the manuscript. All co-authors provided expertise and edits for the manuscript. Dr. William Quinton provided support in conducting field measurements, in discussion of hydrological processes, and in overall guidance on the project. Dr. Xing Fang provided advice and support on the Cold Regions Hydrological Modelling platform, including advice on module performance and parameterizations, edits to the introduction of CRHM in the manuscript and accurate module descriptions in the supplemental materials. Dr. John Pomeroy provided support in module and parameter selection, and generous access to resources to learn CRHM. Dr. Oliver Sonnentag provided expertise on evapotranspiration measured via eddy covariance, including providing access to eddy covariance data his lab group had collected and processed. Dr. Manuel Helbig installed and maintained eddy covariance equipment, and conducted data processing for evapotranspiration data at the bog and landscape scale. He also provided advice for installing eddy covariance equipment in the studied channel fen and performing data processing in EddyPro.

ABSTRACT

Permafrost degradation in the peat-rich southern fringe of the discontinuous permafrost zone is producing substantial changes to land cover with concomitant expansion of permafrost-free wetlands (bogs and fens) and shrinkage of forest supported by permafrost peat plateaus. Predicting discharge from headwater basins in this region depends on understanding and numerically representing the interactions between storage and discharge within and between the major land cover types, and how these interactions are changing. To better understand the implications of land cover change on wetland discharge, the hydrological behaviour of a channel fen in the headwaters of Scotty Creek, Northwest Territories, Canada, dominated by peat plateau-bog complexes, was modelled using the Cold Regions Hydrological Modelling platform for the period of 2009 to 2015. The model performance was evaluated against measured snow depth, snow water equivalent (SWE), evapotranspiration (ET), and water level. The model adequately simulated snowpack dynamics, with root mean square errors (*rmse*) not greater than 11.8 cm for hourly snow depth at a point and 37 mm for annual maximum SWE from snow survey transects. The model generally captured seasonal ET flux and water level fluctuation, with *rmse* less than 0.089 mm/hr and 50 mm, respectively. After model performance evaluation, a sensitivity analysis was conducted to assess the consequences of permafrost loss on discharge from the sub-basin by incrementally reducing the ratio of peat plateau to wetland area in the modelled sub-basin. Reductions in permafrost extent decreased total annual discharge from the channel fen by 2.5% on average for every 10% permafrost loss, due to increased surface storage capacity, reduced runoff efficiency and increased landscape ET. Runoff ratios for the fen hydrological response unit dropped from 0.54 to 0.48 after the simulated 50% permafrost area loss, with a substantial reduction from 0.47 to 0.31 during the snowmelt season. The reduction in peat plateau area also resulted in decreased

intra-annual variability in discharge, with higher low-flows and small increases in subsurface discharge, and decreased peak discharge with large reductions in surface runoff. The current trend of increasing discharge observed in the Scotty Creek basin may not be permanent, as this model shows that a completely connected sub-basin results in decreasing channel fen discharge with further land cover change.

KEYWORDS: wetlands, discontinuous permafrost, discharge, Cold Regions Hydrological Modelling platform, peatlands, land cover change

ACKNOWLEDGEMENTS

No project of this magnitude is created in an intellectual vacuum; there are a number of people I want to thank for their support and input. First and foremost, I would like to thank my thesis advisor, Dr. Bill Quinton. I would never have come to understand the wonderful world of Scotty Creek and all its intricate and interesting details without his unfailing support. He always knew when to push me to do more than I thought I had in me, and allowed me to thrive and become a scientist in my own right.

I would also like to thank the many experts who were involved in the creation of this research and writing of my first academic paper. Dr. John Pomeroy, Xing (Logan) Fang, and the graduate students at the Coldwater Laboratory of the University of Saskatchewan, who gave me the support and resources required to learn the Cold Regions Hydrological Modelling platform and advice on how to improve my modelling efforts. Dr. Oliver Sonnentag and Dr. Manuel Helbig for their expertise on all things evapotranspiration and eddy-covariance related. Dr. Richard Petrone, Dr. Rob Schincariol, and Dr. Brent Wolfe for participating in my thesis defence and providing advice on how to make this document the best representation of my research.

I would like to thank the many graduate students and research assistants who helped me not only understand Scotty Creek and permafrost research, but who also braved the channel fen with me, and who always provided an interesting, or helpfully distracting, discourse in the halls of Laurier: Dr. Ryan Connon, Elise Devoie, Elyse Mathieu, Bhaleka Persaud, Jared Simpson, Olivia Carpino, Joelle Langford, and Caren Ackley.

My family have been incredibly kind and supportive, even when I told them they were no longer allowed to ask me questions like "*how is your thesis going?*", or "*so when do you think*

you'll be done?". Their interest in my work, confidence in my success, and constant love were invaluable to bringing this body of work to completion.

Finally, I would like to thank Scott Duncan. I think it is not hyperbole to say this wouldn't have been possible without you. Your late night discussions and analysis, plans of attack, patience as I practiced every presentation on you, and never-ending love and support got me through to the end, thank you.

TABLE OF CONTENTS

LIST OF TABLES

LIST OF FIGURES

1. INTRODUCTION

This thesis has been organized following the manuscript format to include three chapters. The first chapter is an introduction to the body of work, which includes relevant background research conducted in the Scotty Creek basin and on peatland hydrology, as well as a summary of the objectives and methods used in this study. The second chapter is a complete manuscript that presents the major findings of this research, including more detailed methods, results and discussions. The third and final chapter summarizes the principal findings of the study and presents opportunities for further work. Additional material in the form of water balance and numerical model details are present in a supplementary material chapter at the end of this body of work.

1.1 Literature Review

Hundreds of papers have been written worldwide on the function of individual wetlands in specific environments within the local water cycle. A review of this literature shows that on the global average, wetlands can provide almost any hydrological role (Bullock & Acreman, 2003). The dominant climatological processes in the geographical area of interest provide insight into understanding the hydrological functions of a wetland, as well as understanding soil properties that describe peatlands in general. In the Scotty Creek basin, cold regions processes, and in particular the influence of permafrost and snowmelt, and the extensive coverage of peatlands play crucial roles in understanding the hydrology of the region (Quinton et al., 2009).

In the peatlands of North America, the effects of freezing surface soils may have a larger role than in regions dominated by minerogenic soils (Woo & Winter, 1993). Frozen mineral soils have been shown to allow minimal but measurable infiltration (Alexeev et al., 1972; Gray et al., 1984; Zhao & Gray, 1999), however peatlands may have a significantly higher moisture content

and thus may be seen as virtually impenetrable when frost is consistent at the surface. In some cases, buildup of white ice or the formation of concrete frost occurs at the surface of peatlands as the water table exceeds the wetland surface periodically during freeze up (Price, 1987; Damman, 1986). The energy controls on the development of surface frost is also largely driven by soil moisture content, as water has a much higher heat loss required to initiate freezing than dry peat, regulating the depth and the rate of peatland surface freezing (Farouki, 1981; Woo & Winter, 1993). This heat loss is also controlled by the snow cover timing, extent and snow water equivalent (SWE), as snow acts as an insulator between the peatland surface and the atmosphere (Brown & Williams, 1972). Most significantly, the surface ice in peatlands impedes snowmelt from infiltrating in early spring (Woo & Winter, 1993), contributing to high discharge rates as the wetlands are unable to attenuate high flows (Roulet & Woo, 1986).

Peatlands have two broadly defined layers with significantly different porosities and hydraulic conductivities (Ingram, 1978). The upper layer near the ground surface is commonly referred to as the acrotelm. It is the layer that contains actively growing peat producing vegetation, has air filled pores on a more common basis, and in which the water table typically varies. Below this acrotelm layer is the catotelm, which has a much smaller hydraulic conductivity and typically has smaller variations in water saturation, pore size, and biological attributes (Ingram, 1978). The thickness of the acrotelm varies, particularly with varying peatland surface topography, with depths of up to 50cm where hummocks are present and as little as 10cm in the hollows between them (Damman, 1986). Though thickness may vary with surface topography, overall there appears to be relatively stable acrotelm thicknesses with time that is controlled by negative feedback-loops between water-table elevations and peat formation (Belyea & Clymo, 2001). The vastly different physical properties of peat near the ground surface and deep peat means that the water table does

not react linearly to additional water inputs (Hogan et al., 2006) and long-term draw-down of the water table results in more rapid decomposition of peat impacting the physical properties of the deep peat, reducing the porosity and in turn increasing the water table elevation (Whittington & Price, 2006). Ultimately, the dominant peatland cover type, or microform, and the rate of peat formation change to compensate for changes in water table elevation and water storage.

The Scotty Creek basin has been the site of intense field study to improve our understanding of the heterogeneous peatlands typical of the discontinuous permafrost zone in the Lower Liard River, allowing for better parameterization in hydrological modelling (Pietroniro et al., 1996; Quinton et al., 2003; Quinton et al., 2009). Permafrost in this basin was first developed due to vertical peat accumulation followed by a period of climate cooling (Pelletier et al., 2017), and exists as thin permafrost bodies with steep sides between permafrost and non-permafrost areas (McClymont et al., 2013). Within the Boreal Plains where peatlands are underlain by clay-rich glacial till, groundwater flow is restricted to near-surface, local systems (Ferone & Devito, 2004) and permafrost can acts as a barrier to subsurface contributions between land cover types (Price & Fitzgibbon, 1987). Thus, understanding subsurface contributing area depends on accurately describing the extent and connectedness of Scotty Creek's different peatlands. There exist five major land cover types in the Scotty Creek basin: mineral uplands (48% areal extent), peat plateaus (20%), flat ombrotrophic bogs (19%), channel fens (12%) and lakes (2%) (Chasmer et al., 2014), though in the upper two-thirds of the watershed mineral uplands are less common (Quinton et al., 2003). The basin has undergone rapid land cover change due to permafrost thaw with an estimated 11% decrease in peat plateau area between 1970 and 2008 (Quinton et al., 2011), and the ratio of peat plateau perimeter to area has increased linearly between 1947 and 2008 (Chasmer et al., 2011).

Understanding the hydrological implications of this change depends first on understanding the role of individual land cover types, and second on investigating the interactions between them.

Peat plateaus are elevated features in the landscape due to a permafrost core and they function as runoff generators (Quinton et al., 2003). The peat porosity and saturated hydraulic conductivity decreases with depth with a sharp transition near the division of the acrotelm and catotelm, between 10 and 20 cm depth from the vegetated surface (Quinton et al., 2008). The largest hydrologic event of the year is the spring freshet. When snowmelt occurs, the frost table is within 0.1m of the surface (Quinton & Hayashi, 2005) in the zone of high saturated hydraulic conductivity on the order of 10^3 m/d (Quinton et al., 2008). The snowmelt water forms part of a perched aquifer and is rapidly transported to surrounding wetlands, contributing to high discharge during the freshet (Wright et al., 2008). After snowmelt, plateaus continue to contribute to surrounding wetlands by laterally transporting water through the zone of low saturated hydraulic conductivity, though rain can sufficiently raise the water table in order to result in rapid movement (Quinton & Baltzer, 2013). As permafrost thaws, peat plateaus undergo both vertical and lateral thaw (Quinton et al., 2011). At the thawing edges of peat plateau there is a rapid change in vegetation structure as black spruce trees, the dominant vegetation on peat plateau, are intolerant to flooding (Baltzer et al., 2014; Chasmer et al., 2011; Patankar et al., 2015). At the edges of peat plateaus permafrost thaw results in surface subsidence which results in higher moisture content in the peat. When black spruce tree roots are in sufficiently high moisture content the roots are no longer able to function (Baltzer et al., 2014; Patankar et al., 2015). Deteriorating root function in turn affects tree viability due to overall decreases in transpiration rates leading to tree mortality and reduced canopy extent (Chasmer et al., 2011). The resultant increase in shortwave radiation reaching the ground surface increases ground temperature and further contributes to permafrost

thaw. The combination of these positive feedbacks results in increased permafrost fragmentation and net forest loss (Baltzer et al., 2014). Vertical permafrost thaw not only results in forest loss and plateau fragmentation, but lateral permafrost thaw results in decreased plateau runoff due to lowered hydraulic gradients and thickening of the active layer (Quinton & Baltzer, 2013). Modelling of complete forest loss due to permafrost degradation replaced by a homogeneous wetland landscape concluded that in the long term, forest loss may result in changing precipitation inputs and climatic cooling due to changes in the boundary layer heights in the summer, which may be sufficient to slow down the effects of climate warming (Helbig et al., 2017b).

In the Scotty Creek basin, wetlands either take the form of flat bogs or channel fens. Bogs in this basin are either hydrologically isolated from the drainage network that act as storage features (Quinton et al., 2003) or may form part of a bog cascade (Connon et al., 2014). Bog cascades may be seasonally connected to the drainage network when soil moisture conditions are sufficiently high, typically during the snowmelt season, by connecting through ephemeral flow through features that cut through adjacent permafrost bodies. After snowmelt, the combined effect of thawing surface ice leading to infiltration, and the draw-down of the water table because of evapotranspiration, can create a storage deficit that temporarily disconnects a bog, or a series of bogs connected leading to an unconnected bog, from the drainage network (Connon et al., 2015). In this way, the bog cascades may behave similarly to the 'element threshold' concept developed by Spence and Woo (2006), where the Scotty Creek basin has a variable contributing area dependent on moisture conditions. As permafrost thaw increases and peat plateaus give way to flat bogs and channel fens, basin contributing area is expected to increase (Connon et al., 2015).

Channel fens are wide, linear wetlands that connect in a dendritic pattern between lakes, acting as flow through features to laterally convey water to the basin outlet (Quinton et al., 2003).

Roughness based routing algorithms have been shown to accurately represent flow conditions in a channel fen, with manning's roughness values of n=0.13 to 0.17 (Quinton et al., 2003). Isotopic composition of water in a channel fen was similar to an upstream lake during high flow conditions and similar to adjacent peat plateaus during low flow conditions, suggesting the channel fen may become hydrologically disconnected from the upstream lake and receive no lake outflow under sufficiently low moisture conditions (Hayashi et al., 2004).

There is a network of linear disturbances in the Scotty Creek basin in the form of old, unused winter roads and cut lines from seismic exploration (Williams et al., 2013). These linear disturbances cross all previously described land cover types, removing the tree cover from peat plateaus. The loss of tree cover in these linear disturbances results in increased radiation at the ground surface contributing to permafrost degradation (Quinton et al., 2009; Chasmer et al., 2011), though the use of mulching practices has been shown to reduce to rate of permafrost degradation (Mohammed et al., 2017). Permafrost degradation may potentially short-circuit the existing drainage network by removing permafrost dams which impede flow between bogs and fens, either by connecting previously isolated bogs or by providing a shorter path than an existing cascade (Quinton et al., 2011). Hydrologic connectivity between bogs and channel fen through a seismic line crossing a peat plateau has been observed with hydraulic gradients moving water from the bog to the fen, from the fen to the bog, and from the crossed peat plateau to both the fen and the bog (Braverman & Quinton, 2016). However, a study of seismic lines including DEM analysis found that overall there was a low connectivity between adjacent wetlands due to linear disturbances (Williams et al., 2013). An in-depth study of one seismic line in particular found that the seismic line behaved more similarly to a bog than a channel fen, as it was seasonally connected through surface pathways and only contributed to the channel fen from upstream bogs and peat plateaus

during the snowmelt period (Williams et al., 2013). Williams et al. (2013) concludes that though the density of seismic lines is five times higher than the density of the natural drainage network (Quinton et al., 2011) the studied linear disturbances appear to have not increased the basin's hydrological connectivity.

Permafrost degradation and the associated hydrological changes also have the potential to impact nutrient, carbon and energy cycling in the Scotty Creek basin. Mercury and methylmercury are found in greater concentrations in downstream bogs within bog cascades, suggesting that as the basin becomes increasingly connected there will be an increased number of features that are hotspots for mercury methylation that can contribute to downstream ecosystems (Gordon et al., 2016). Hydrology and carbon export are tightly linked in peatlands (Holden, 2005). Wetland expansion in Scotty Creek can increase basin methane emissions sufficiently that estimated increases in boreal forest carbon dioxide uptake will not offset the net greenhouse gas forcing (Helbig et al., 2017a; Helbig et al., 2017b), though methane emissions may also increase without wetland expansion due to increasing spring soil temperatures (Helbig et al., 2017c). Analysis of peat cores suggests that permafrost periods have slower carbon accumulation rates than non-permafrost periods for both bogs and plateaus (Pelletier et al., 2017), but that the lower carbon accumulation rates during permafrost periods may be compensated in the long term by varying decomposition rates of peat types on plateaus. Wetlands have increased radiation energy inputs at their surface compared to plateaus, and increasing wetland area means increased radiative energy inputs at the basin scale. This energy can then influence lateral permafrost thaw through subsurface heat transfer associated with groundwater flow (Kurylyk et al., 2016), leading to even further increased wetland area. Vegetation cover, energy inputs, hydrology, permafrost degradation and land cover change are all tightly linked in the Scotty Creek basin.

1.2 Objectives

The primary objectives of this research are to improve the understanding of how channel fens in the discontinuous permafrost zone may respond to further wetland expansion with permafrost-loss driven land cover change. Therefore, the research objectives are as follows:

1. Develop a conceptual model for a channel fen that includes the seasonally dominant hydrological processes in the Scotty Creek basin,
2. Develop a numerical model of the discharge from a channel fen using the Cold Regions Hydrological Modelling platform, and
3. Perform a sensitivity analysis of the consequences of permafrost loss on the discharge from a channel fen by incrementally reducing the forest peat plateau area in the model and increasing the wetland area as either channel fen or bog.

1.3 Methods

A channel fen in the Scotty Creek basin (Figure 1b) was intensively instrumented in order to conduct a detailed water balance analysis that could be used to inform a conceptual model of the hydrology of channel fens in the region. The studied channel fen (Figure 1c) covers a straight distance of approximately 600m connecting the upstream Goose Lake to the downstream First Lake. Hydrological data were grouped into three components for the water balance, discharge into the fen, discharge out of the fen, and atmospheric fluxes.

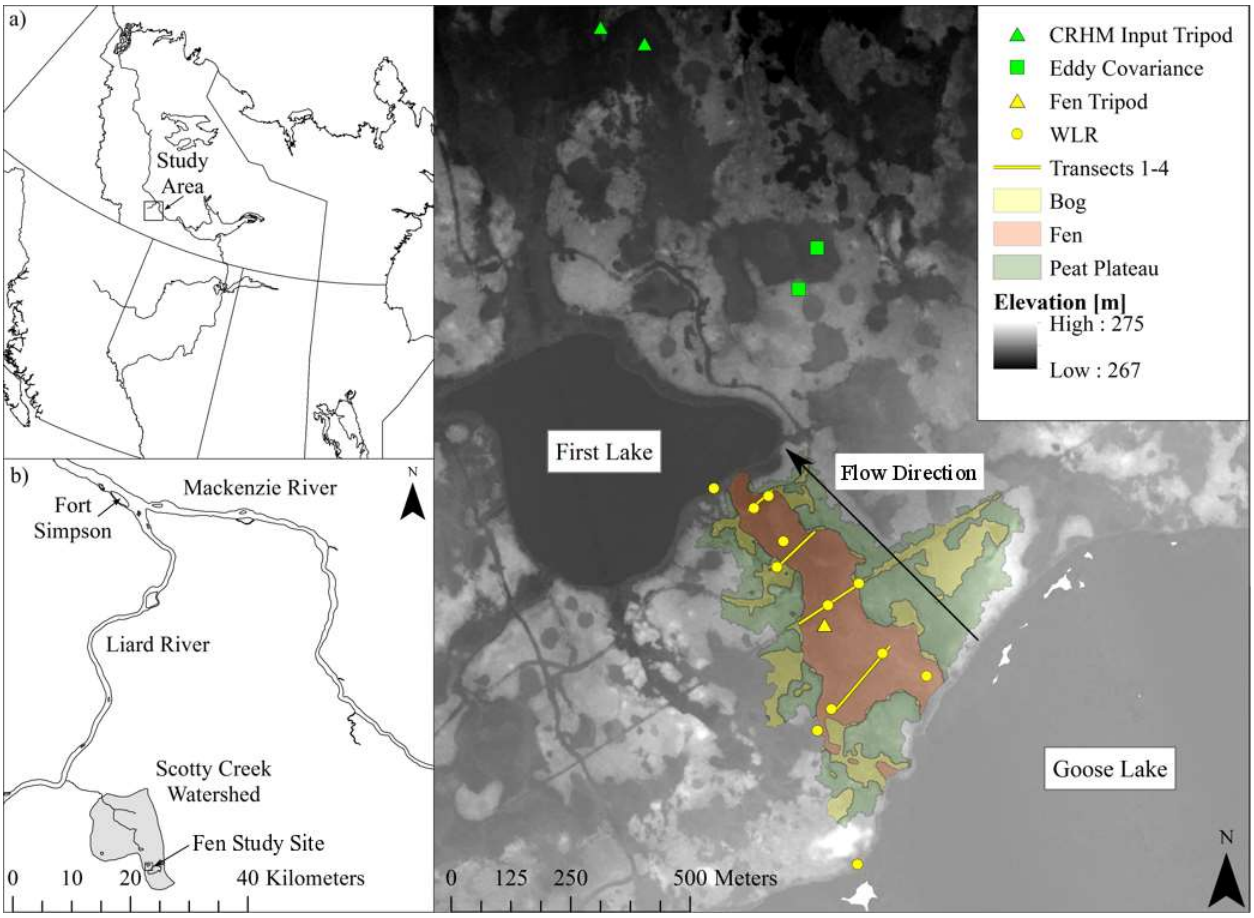

Figure 1. a) Study area within the Northwest Territories, b) the Scotty Creek basin, and c) the studied channel fen (red) including land cover types, equipment locations and elevation from Light, Imaging Detection, And Ranging survey (LiDAR). Equipment locations (e.g. eddy covariance, meteorological tripods) in green were used for numerical modelling in Cold Regions Hydrological Modelling platform (CRHM) and performance evaluation. Equipment locations (e.g., water level recorders, and meteorological tripod) within the channel fen watershed in yellow were part of the water balance calculations performed to develop the conceptual model.

A meteorological tripod was set up (Figure 1c) to measure four-component radiation, air temperature, relative humidity, wind speed, depth to snow surface, and ground temperature every half hour in the studied channel fen. The tripod was also equipped with eddy covariance equipment (hydrometer, 3d sonic anemometer) to measure evapotranspiration between April and the end of August. Hourly precipitation measurements were recorded at a nearby Geonor weighing gauge, whose data was corrected for wind undercatch. Water level recorders were installed in the

upstream and downstream lakes, along the center of the channel fen, and in adjacent hydrologically connected features (open bogs, seismic line, abandoned winter road). Four transects (T1through T4, Figure 1c) were established that cross the fen surface perpendicular to the direction of flow in order to measure snow depth and density, water depth and velocity, and depth to seasonal frost. Transects were oriented such that all characteristic vegetation types on the fen were included when measuring snow, water and frost variables, as well as extending into open connected features on each transect. Two ablation stakes were established along each of the four transects, one in an area representing the channel fen and one representing an open connected feature. The ablation stakes were supplemented with snow depth and density surveys conducted three times weekly at the end of the snow accumulation season and throughout the spring freshet to establish the rate of snowmelt. Once the snowcover on the fen was depleted, water depth and velocity were monitored three times weekly using an acoustic Doppler system until water velocities were below the ability of equipment to detect. The depth of seasonal frost was monitored post snowmelt using a frost probe at all transect points weekly during the first month after snowmelt, or until the seasonal frost had disappeared. The location and elevation of all transect points and equipment was recorded using a Differential Global Positioning System.

The conceptual model derived from the above water balance and hydrological measurements was used in combination with previously published field studies in Scotty Creek to inform a numerical model. CRHM was used to build a hydrological model of the channel fen in order to model discharge out of the channel fen. Modules descriptions and parameter sources are available in the supplemental materials chapter. The model's performance was evaluated by comparing modeled values against snow depth, snow water equivalent, evapotranspiration, and water level measured in multiple HRUs as there existed no record of wetland discharge to use for

validation (Table I). The proportion of peat plateau in the model was incrementally reduced and replaced by either bog or wetland area according to four wetland-area-increase scenarios,

I. All lost plateau area becomes bog (Scenario “All Bog”),

II. the ratio of channel fen–to-bog area of the 2010 HRU delineation in the modelled sub-basin is maintained, with expanded wetland area added at a ratio of 1.63:1 fen to bog (Scenario “Sub-Basin”),

III. the ratio of fen-to-bog area of the greater Scotty Creek watershed is used to determine the ratio at which simulated lost plateau area is replaced, with expanded wetland area added at a ratio of 1.92:1 fen to bog (Scenario “Scotty”),

IV. all simulated peat plateau reduced area is replaced by expanded fen area (Scenario “All Fen”).

These four scenarios were run for three increments of prescribed permafrost loss, 10% less permafrost than the extent in 2010, 25% less and 50% less. Runoff ratios were calculated to illustrate the changing hydrologic behaviour of the basin.

2. Modelling the effects of permafrost loss on discharge from wetland dominated basins in the discontinuous permafrost zone

L.E. Stone[1*], W.L. Quinton[1], X. Fang[2], J.W. Pomeroy[2], O. Sonnentag[3], M. Helbig[3]

[1] Cold Regions Research Centre, Wilfrid Laurier University, Waterloo, ON, N2L 3C5

Phone: 226-791-7025 , E-mail: ston5270@mylaurier.ca

[2] Centre for Hydrology, University of Saskatchewan, Saskatoon, SK, S7N 5C8

[3] Département de Géographie, Université de Montréal, Montréal, QC, H3C 3J7

2.1 ABSTRACT

Permafrost degradation in the peat-rich southern fringe of the discontinuous permafrost zone is producing substantial changes to land cover with concomitant expansion of permafrost-free wetlands (bogs and fens) and shrinkage of forest supported by permafrost peat plateaus. Predicting discharge from headwater basins in this region depends on understanding and numerically representing the interactions between storage and discharge within and between the major land cover types, and how these interactions are changing. To better understand the implications of land cover change on wetland discharge, the hydrological behaviour of a channel fen in the headwaters of Scotty Creek, Northwest Territories, Canada, was modelled using the Cold Regions Hydrological Modelling platform for the period of 2009 to 2015. The model performance was evaluated against measured snow depth, snow water equivalent (SWE), evapotranspiration (ET), and water level. The model adequately simulated snowpack dynamics, with root mean square errors (*rmse*) not greater than 11.8 cm for hourly snow depth and 37 mm for annual maximum SWE. The model generally captured seasonal ET flux and water level fluctuation, with *rmse* not greater than 0.089 mm/hr and 50.2 mm, respectively. After model performance evaluation, a sensitivity analysis was conducted to assess the impact of permafrost

loss on discharge from the sub-basin by incrementally reducing the ratio of peat plateau to wetland area in the modelled sub-basin. Reductions in permafrost extent decreased total annual discharge from the channel fen on average by 2.5% for every 10% permafrost loss, due to increased surface storage capacity, reduced runoff efficiency and increased landscape ET. Runoff ratios for the fen hydrological response unit decreased from 0.54 to 0.48 after the simulated 50% permafrost area loss, with a reduction from 0.47 to 0.31 during the snowmelt season. The reduction in peat plateau area also resulted in decreased intra-annual variability in discharge, with higher low-flows and small increases in subsurface discharge, and decreased peak discharge with large reductions in surface runoff. The current trend of increasing discharge observed in the Scotty Creek basin may not be permanent, as this model shows that a completely connected sub-basin results in decreasing channel fen discharge with further land cover change.

2.2 INTRODUCTION

Northwestern Canada has experienced rapid climate warming with air temperatures increasing at twice the rate than the global average (IPCC 2014). Shallow permafrost temperatures have increased across Canada (Smith et al., 2005; Taylor et al., 2006), which has resulted in widespread loss of permafrost in the discontinuous and sporadic permafrost zones and the rate of such losses is accelerating in northwestern peatlands (Camill, 2005). Permafrost degradation has significant impacts on the hydrology in the northwestern permafrost-dominated region of Canada. For example, studies have highlighted increasing baseflow across the Northwest Territories (St Jacques & Sauchyn, 2009), changes in the rate of catastrophic lake drainage (Marsh et al., 2009), and widespread land cover changes with thermokarst development as surface vegetation changes from boreal forest to extensive wetlands (Jorgenson et al., 2001; Quinton et al., 2009). Geochemical analyses in western Siberia highlight a shift from a surface water-dominated system

to groundwater-dominated system with increased mean air temperature and resultant permafrost degradation (Frey et al., 2007). Modeling applications have shown how a decrease in intra-annual variability composed of an increase in base flow and a decrease in peak flow serve as a useful indicator of permafrost degradation in basins based on hydrometric data alone (Frampton et al., 2013). Changes in the hydrology affect other key ecosystem processes such as carbon dynamics (Dimitrov et al., 2014; Helbig et al., 2017a; O'Donnell et al., 2012), transport of nutrients (Frey & McClelland, 2009) and toxins (Gordon et al., 2016), and ground thermal regimes (Sjöberg et al., 2016).

In the peatland-dominated southern margin of discontinuous permafrost of northwestern Canada (Kwong & Gan, 1994), the impact of permafrost degradation is tightly linked to ecological change. Examples of this impact are well illustrated by the Scotty Creek watershed. Peat plateaus are raised by 1-2m above the surrounding wetlands and the local water table due to an ice-rich permafrost core, and are covered by black-spruce dominated boreal forest (Quinton et al., 2003). When this permafrost core thaws, the ground surface subsides and is flooded by the adjacent wetlands (bog or fen). Black spruce trees at the edge of thawing permafrost respond poorly to increased wetness as measured by sap flow in root systems and radial growth of trees (Baltzer et al., 2014; Pantakar et al., 2015), where waterlogged roots cease to function entirely, eventually leading to reduced tree cover and a transition from forest land cover to wetland. As permafrost thaw proceeds, the proportion of the landscape occupied by peat plateaus decreases and as a result so does the proportion of landscape runoff generated by these features. Runoff from thawing peat plateaus also decreases over time since thaw induced ground surface subsidence reduces the hydraulic gradient driving flow (Quinton & Baltzer, 2013). Since the major land cover types of bog, fen and peat plateau each have a specific function in the water balance of basins (Quinton et

al., 2003), a change in their relative proportion may affect the basin hydrograph. Permafrost thaw has increased hydrological connectivity among wetlands. For example, bogs that were once hydrologically isolated have developed ephemeral connections with other such bogs so that collectively they cascade water from one bog to the next and eventually into the channel fen from where it is routed to the basin outlet. This thaw-induced increased connectivity of wetlands has expanded the runoff contributing area of drainage basins, a process that offers a plausible explanation for the rising discharge from basins observed throughout the southern fringe of permafrost in northwestern Canada (Connon et al., 2014).

Predicting basin discharge in this region depends first on understanding the individual impacts of permafrost degradation on the major land cover types, and second on understanding the hydrological interactions between the major land cover types. Significant improvements have been made in our understanding of the hydrological contributions from peat plateaus (Wright et al., 2008; Quinton & Baltzer, 2013) and bogs (Connon et al., 2015) to channel fens with on-going permafrost degradation. However, our understanding of the system needs improvement on two topics. First, there exists no conceptual model of how channel fens store and transport water, though they are understood to function as lateral transport of water to the basin outlet (Quinton et al., 2003) and roughness based algorithms were determined to be appropriate for approximating surface discharge (Hayashi et al., 2004). Secondly, current studies on permafrost degradation in the discontinuous permafrost zone are operating under the framework of expanding contributing area through thaw-induced increases in hydrologic connectivity. However, there is an upper limit to how much the contributing area can expand. Once all bogs form part of a cascade, and all areas are able to contribute to the basin, how might discharge from channel fens change?

Wetlands can have a wide variety of hydrological functions, with wetlands contributing to both reduction and augmentation of floods and peak flows depending on their particular environmental and climatic conditions (Bullock & Acreman, 2003). It is therefore crucial to study the seasonally dominant functions of channel fens in Scotty Creek before attempting to numerically model their discharge. Improving our understanding of channel fens with a detailed water balance, combined with previous works on bog cascades and on peat plateaus, provides the opportunity to represent the fen-bog-peat plateau complex in a numerical model. Physically-based hydrological models are useful for testing the impacts of land cover and climate change on hydrological variables. The Cold Regions Hydrological Modelling (CRHM) platform has been successfully applied to simulate hydrological processes in many Canadian regions (Pomeroy et al., 2007), such as northern Canada (Dornes et al., 2008; Rasouli et al., 2014; Krogh et al., 2017), the Canadian prairies (Fang et al., 2010; Cordeiro et al., 2017; Mahmood et al., 2017), and the Canadian Rockies (Fang et al., 2013; Pomeroy et al., 2016) as well as globally, in China (Zhou et al., 2014), Patagonia (Krogh et al., 2015), the Pyrenees (Lopez-Moreno et al., 2012) and the German Alps (Weber et al., 2016). CRHM has also been used for sensitivity analysis to assess the impact of changing climatic conditions on snowpack development (Lopez-Moreno et al., 2012), the impact of forest cover on snowmelt hydrology (Pomeroy et al., 2012), and the impact of antecedent conditions on the Alberta June 2013 flood in a mountainous headwater basin (Fang & Pomeroy, 2016). CRHM was selected for the purposes of this study because of its widespread successful applications, its concentration on cold regions processes, and its relatively simple input data requirements.

Here we aim to improve the understanding of how permafrost thaw driven conversion of forest to wetland affects the hydrology of channel fens. This will be achieved through the following

specific objectives: (i) develop a conceptual model for a channel fen of the seasonally dominant hydrological processes; (ii) develop a numerical model of the discharge from a channel fen using CRHM; and (iii) perform a sensitivity analysis of the impact of permafrost loss on the discharge from a channel fen by incrementally reducing the area of permafrost-underlain peat plateau in the model and increasing the area of permafrost-free channel fen and bog.

2.3 STUDY SITE

Scotty Creek is a 152 km^2 biophysically representative basin for the lower Liard River valley in the Northwest Territories, Canada. The basin is in the southern fringe of the discontinuous permafrost zone, approximately 50 km south of Fort Simpson (Figure 1a, 1b). Approximately 40% of the basin is underlain by shallow permafrost (<10 m thick) (Burgess & Smith, 2000; Quinton et al, 2011). Daily average air temperature (1981-2010) recorded at the Fort Simpson airport is -2.8 °C, with average air temperatures of -24.2 °C for January and 17.4 °C for July. The region receives an average of 388 mm of precipitation annually, of which 187 mm falls as snow (Environment and Climate Change Canada, 2017). Elevation in the basin ranges from 210 m to 285 m above sea level, with an average gradient of 0.0032 m/m (Quinton & Hayashi, 2008). The majority of the basin has deep peat deposits (2-8 m) underlain by a clay-rich glacial till with occasional sandy mineral uplands (Aylsworth et al., 2000).

The headwater portion of the basin is characterized by large wetland areas interspersed with raised, forested peat plateaus and small lakes (Quinton et al., 2003). There are four major land cover types in this portion of the basin: peat plateau, channel fen, bog, and lake. Detailed descriptions of land cover function can be found for peat plateaus (Wright et al., 2008), and bogs and bog cascades (Connon et al., 2015). However, only more preliminary studies have been performed on channel fens (Quinton et al., 2003). In Scotty Creek, the areal portion of land cover

types is approximately 20% peat plateau, 12% fen, 19% bog and 3% lake, with 43% of the area as mineral uplands, which are predominantly absent in the wetland dominated headwaters (Chasmer et al., 2014; Quinton & Hayashi, 2008). The basin has seen a rapid decrease in permafrost area; 38% of peat plateau area was converted to wetlands between 1947 and 2008 (Quinton et al., 2011). This study focuses on one channel fen, which covers a straight distance of approximately 600 m between a source lake (Goose Lake) and outlet lake (First Lake, Figure 1c). The fen was selected as it had well-defined edges with a limited number of hydrologically-connected contributing areas, including peat plateaus, bogs, and two linear disturbances (a cut line from seismic exploration and an abandoned winter road), was nearby long term meteorological measurements, and was accessible from the Scotty Creek research facilities. Peat depth in the fen ranges between 3.0 to 4.5 m and is underlain by clay-rich glacial till with a relatively low hydraulic conductivity. The fen is considered representative of the land cover type in the basin as a whole, with an average flood-wave velocity of 0.11 km/hr which is equal to the reported celerity of a headwater fen in Quinton et al. (2003) and average measured surface velocity of 0.032 m/s compared to 0.02 m/s in Quinton et al (2003).

2.4 METHODS

2.4.1 Instrumentation

A water level recorder network (Solinst Levelogger Gold, Hobo U20L-04) was installed in the center of the channel fen (Figure 1c) as well as in all non-forested connected features (for example, bogs and linear disturbances) in late August 2014, recording every minute and calculating half-hourly averages. This water level recorder network was operational overwinter 2014-2015 as it was installed significantly below freezing depths (>1 m). Water level recorders

were anchored to black iron pipe, which had been hammered into the underlying mineral soil to prevent mire breathing from moving sensors (Fritz et al., 2008).

Hourly total precipitation data were recorded using a Geonor T-200B weighing gauge installed in August 2008 with no overhead canopy and serviced bi-annually. Geonor data were corrected using the R programming language and environment used for statistical computing (R Core Team, 2017).The CRHMr R package (Shook, 2016) was used to correct recorded jitter, the function's automated filtering of noise in Geonor data are described in Pan et al. (2016). Precipitation data were then corrected for undercatch by determining precipitation type from hydrometeor temperature and adjusting for the catch efficiency (CE) of the gauge depending on wind speed (Ws) measured at the height of the altar shield (Harder & Pomeroy, 2013; Smith, 2007).

$$P_{corrected} = \frac{P_{obs}}{CE}, CE = 1.18e^{-0.18Ws} \quad (1)$$

In April 2015, a meteorological tripod was set up in a central location on the fen. It was equipped to measure four-component radiation (CNR4, Kipp and Zonen, Delft, the Netherlands), air temperature and relative humidity (HC-S3-XT, Rotronic Hygroclip, Switzerland), wind speed (05103, R.M. Young Wind Monitor, United States of America), depth to snow surface (SR50, Campbell Scientific Canada, Edmonton, AB), and ground temperature (109, Campbell Scientific Inc, Logan, UT, USA, installed every 15 cm between 0 cm and 75 cm below the vegetated surface) every half-hour. Evapotranspiration from the fen (ET_{fen}) was measured using high frequency eddy covariance equipment installed on the fen meteorological tripod (Figure 1c) taking measurements at a 10 Hz frequency between 09/04/2015 and 25/08/2015. The 3D wind velocities were measured using a sonic anemometer (CSAT, Campbell Scientific Inc, Logan, UT, USA), and the changes in atmospheric water vapor were measured using a krypton hygrometer (KH20, Campbell Scientific

Inc, Logan, UT, USA). Latent heat fluxes were calculated using the EDDYPRO software (version 6.1.0; LI-COR Biogeosciences). Eddy covariance data processing included the following steps: the sonic anemometer tilt was corrected using double rotation, spikes were removed in the high frequency time series using the method developed by Vickers & Mahrt (1997), high frequency ET_{fen} data were block-averaged for an hourly time series, and covariance maximization was used to compensate for time lags (Fan et al., 1990),

Evapotranspiration (ET) was also measured for a bog (ET_{bog}) and for the landscape (ET_{land}), which were derived from eddy-covariance instruments as described by Helbig et al. (2016) and Warren et al. (2017). A tripod located in a large open bog (Figure 1c) was instrumented with eddy-covariance equipment (CSAT3A & EC150, Campbell Scientific) in 2014, and was used to evaluate the performance of the summertime modelled ET_{bog} in 2014 and 2015 for the bog HRU. A 15m meteorological tower (Figure 1c) was equipped with the same eddy-covariance instrumentation above the forest canopy in 2013. The eddy covariance flux footprint resulted in a landscape-scale measurement of the combined ET_{land} of bog and peat plateau areas during the summer in 2013, 2014 and 2015; no fen area is included in this measurement. Details regarding instrument set-up and processing of ET_{bog} is described in Helbig et al. (2017b). Details regarding the derivation of landscape ET_{land} is in Warren et al. (2017). Flux footprint data quantifies the percent-bog and percent-peat plateau contribution to the half-hourly ET_{land} measurements (see Helbig et al., 2016). Modelled bog and peat plateau ET values were combined using the same contributions as the reported footprint model-derived percent-contributions to create a modelled ET_{land} (Warren et al., 2017). For all years and for the ET_{bog} and ET_{land} measurements, modelled results were compared against measured hourly values for days with at least 75% measurement data coverage.

Data from two meteorological tripods that were established in 2004 were compiled for CRHM modelling (August 2008-August 2015, locations of tripods in Figure 1c). Data from a tripod erected in an open bog were used to represent input data for modelled bog, channel fen and lake area; separate input data were used for the peat plateau from a meteorological tripod installed below the canopy on a peat plateau. Input data included average hourly incoming shortwave radiation (CNR1, Net Radiometer, Campbell Scientific, Logan, UT, USA), wind speed (031A, Met One Wind Speed Sensor, Campbell Scientific, Logan, UT), relative humidity and air temperature (HMP45C, Temperature and Relative Humidity Probe, Vaisala Inc, Helsinki, Finland). Data gaps less than three hours were filled using linear interpolation. Data gaps longer than three hours were filled using measurements from other meteorological stations located on similar land cover types from the Scotty Creek network of meteorological stations. The tripods also included a Sonic Ranging Sensor (SR50A, Campbell Scientific, Logan, UT, USA). Annual manual measurements of the distance from the sensor to the snow surface were conducted at the end of the snow accumulation season to validate sensor recordings. Missing snow depth above 8 cm were gap filled with the most recently recorded values. Snow depth measurements below 8 cm had poor quality signal values. Snow depth measurements below 8 cm were considered 0 cm. In 2010, the SR50 sensor installed on the bog tripod was replaced after multiple malfunctions; data between servicing of the bog tripod in 2009 and replacement of the sensor in 2010 were removed from the analysis.

The water table was recorded in the bog using a vented water level recorder (WL16s, Water Level Logger, Global Water Instrumentation, Sacramento, CA, USA, 2008-2013) and a non-vented water level recorder corrected using a separate barometric logger (3001, Levelogger Gold, Solinst, Georgetown, ON, Canada, 2014-2015) in the bog where the meteorological tripod was

located (Figure 1c). Sensors were installed annually in the early summer after snowmelt and after the surface of the bog had thawed, and were removed before soil freezing in the fall. The depth to water table, depth to sensor tip, and depth to ground surface from the top of the well were measured at install and removal.

2.4.2 Water Balance

Four transects (T1through T4, Figure 1c) were established in late August 2014 that cross the fen surface perpendicular to the direction of flow in order to measure snow depth and density, water depth and velocity, and depth to seasonal frost. All variables were measured approximately every 5 m, except for snow density which was measured every 25 m. Transects are separated by an average of 140 m, with total distances of 175 m, 140 m, 105 m and 65 m of Transects 1 through 4, respectively. Transects were oriented such that all characteristic vegetation types on the fen were included when measuring snow, water and frost variables, as well as extending into open connected features on each transect. In early March 2015, two ablation stakes were established along each of the four transects, one in an area representing the channel fen and one representing an open connected feature. The ablation stakes were supplemented with snow depth and density surveys conducted three times weekly at the end of the snow accumulation season and throughout the spring freshet to establish the rate of snowmelt. Once the snowcover on the fen was depleted, water depth and velocity were monitored three times weekly using an acoustic Doppler system (SonTek, FlowTracker, San Diego, CA, USA) until water velocities were below the ability of equipment to detect. The depth of seasonal frost was monitored after snowmelt using a frost probe at all transect points weekly during the first month after snowmelt, or until the seasonal frost had disappeared. The location and elevation of all transect points and equipment was recorded using a Differential Global Positioning System (DGPS, Leica GS10 RTK GPS, Switzerland).

On days where eddy covariance data were not available, the Priestley-Taylor (Priestley & Taylor, 1972) method was used to estimate ET_{fen} from the fen surface. ET_{fen} is assumed to be zero during the "winter" period, between 18/12/2014 and 04/03/2015. If less than 75% of hourly block-average eddy covariance data were available, then the Priestley-Taylor method was used to estimate daily ET_{fen}.

Measurements of water level, snowmelt, rainfall and ET_{fen} were used to compute a channel fen water balance (equation 2). This was done by partitioning fluxes into three components: discharge into the fen, discharge out of the fen, and the atmospheric flux.

$$S = (Q_{sub}IN + Q_{sur}IN) - (Q_{sub}OUT + Q_{sur}OUT) + (P_r + P_s - ET) \quad (2)$$

where S [mm/day] is the change in storage in the channel fen, Q [mm/day] is the discharge of water into or out of the fen calculated separately for the surface discharge and the subsurface discharge, P_s [mm/day] is snowmelt added at the fen surface, P_r [mm/day] is rainfall, and ET [mm/day] is loss to the atmosphere through ET_{fen}. Incoming discharge was calculated as the input into the channel fen from Goose Lake, as well as the input of the bog connected on T1, the seismic line connected on T2, the small bog connected on T3, and the winter road connected on T4 (Figure 1c). Outgoing discharge was the output from the channel fen to First Lake. Due to the low hydraulic conductivity of the underlying glacial till layer, deep groundwater flow was considered to be a net zero flux, with no vertical loss or gain. Details on calculation of surface discharge (Manning's equation) and subsurface discharge (Darcy's law) is included in the supplemental materials.

For the purposes of discussion, four time periods were assigned; the "spring" period between 04/04/2015 and 31/05/2015 whose start date is defined by the first observation of snowmelt in the channel fen during field studies and whose end date is determined by when the water level in the fen reached a relatively stable height of within 5 cm above the fen surface, the

"summer" period between 01/06/2015 and 26/08/2015 defined as the time period after water table stabilization that occurred with the end of the spring freshet and ending when data collection ended in 2015, the "fall" period between 02/09/2014 and 17/12/2014 whose start date is defined by the beginning of data recording in the channel fen and whose end date is defined by the first time period where frozen ground was recorded at the bog tripod from a temperature probe installed at 10 cm below the vegetated surface, and the winter period between 18/12/2014 and 04/03/2015 defined as the remaining time interval between previously defined "fall" and "spring" periods.

2.4.3 Numerical Model Description - CRHM

CRHM is a flexible, process-based, modular modelling platform (Pomeroy et al., 2007). It uses the Hydrological Response Unit (HRU) concept to permit flexible basin discretization from lumped to finely distributed and requires continuous forcing data including temperature, relative humidity, wind speed and precipitation. A library of modules is available to model hydrological processes, with a focus on processes crucial to cold regions (e.g., snow transportation, interception, sublimation and melt, infiltration into frozen soils, ground freeze and thaw), however a full range of non-cold regions modules are available. A basin-specific model application is built by selecting appropriate modules based on the basin of interest. Modules must then be parameterized based on field observations, from literature or by calibration.

CRHM was used to model the hydrology of a small sub-basin (0.45 km^2) representative of the peat plateau-bog-channel fen complex found in the headwaters of Scotty Creek. Model modules were selected to reflect the cold region processes outlined in the conceptual model developed from the water balance calculations and field studies (Figure 2, module descriptions and parameter sources in supplemental materials). The modelled sub-basin represents the hydrology of the channel fen, which connects Goose Lake and First Lake (Figure 1c). The

watershed for the channel fen was determined through spatial analysis using the ArcMap Spatial Analyst/Hydrology toolbox using the 2010 LiDAR derived DEM as input (Chasmer et al., 2010). Due to the low topographic gradients of the headwaters of the Scotty Creek basin, there is little difference in slope, elevation or aspect across the modelled sub-basin. Land cover type has been shown to be the most important factor leading to different hydrological processes (Quinton et al., 2003). The HRUs for the modelled sub-basin were determined from a land cover classification map of the Scotty Creek watershed based on 2010 LiDAR data collection (Chasmer et al., 2014), therefore the baseline model run is representative of the 2010 permafrost extent, covering 112,600 m^2 or 25% of the modelled sub-basin area. Four HRUs were defined in this model: peat plateau, bog, fen and lake. In this study, all bogs within the watershed of the channel fen are considered hydrologically connected to the channel fen and the entire modelled sub-basin is considered a contributing area. The model simulates snow interception and sublimation from forest canopies, energy balance snowmelt, evapotranspiration, peat soil water storage and transmission, frost table dynamics, and runoff by surface, subsurface and groundwater flows above the clay-rich layer. Model parameters were determined from field observations, spatial analysis of the 2010 LiDAR-based DEM, or derived from field studies at Scotty Creek (parameters and sources included in the supplemental materials). The model was driven by a continuous hourly time series of incoming shortwave radiation, wind speed, relative humidity, air temperature and precipitation (instrumentation described above).

Table I. Measured data used for performance evaluation.

Variable	HRU	Dates	Continuous?
Snow Depth [mm]	Plateau	Aug 2008-Aug 2013	Yes, SR50 (Campbell Scientific Canada, Distance Sensor)
	Bog	Aug 2008-Aug 2015	
SWE [mm]	Plateau	Mar 2009-Mar 2015	No, annual snow survey
	Bog	Mar 2009-Mar 2014	
ET [mm/hr]	Landscape	Apr 2014-Dec 2015	Seasonally, measurement details in Helbig et al. (2016)
	Bog	May 2013-Dec 2015	
Water Level [mm]	Bog	June 2009-Aug 2015	Seasonally, water level recorder

No discharge measurements exist for the channel fen to use for validation. Instead, four key hydrological variables were used to evaluate model performance: point snow depth, transect-based snow water equivalent (SWE), point ET and point water table. Table 1 outlines availability of performance evaluation data according to HRU. Table 2 lists four statistics used to evaluate model outputs: mean error (*me*), percent bias (*pbias*), root mean square error (*rmse*), and normalized root mean square error (*nrmse*), as well as the number of values (*n*). The equations used to calculate these statistics are outlined in Table 3. Statistics were calculated using the "hydroGOF" package available for R (Zambrano-Bigiarini, 2014). Additionally, model outputs were evaluated using graphical goodness-of-fit measures, including r-squared values associated with the linear regression of paired values represented in one-to-one plots and Nash-Sutcliffe Efficiencies (*nse*) for time series where applicable.

Table II. Summary of statistics used to evaluate performance of model.

Variable	HRU	*me*	*pbias* %	*rmse*	*nrmse* %	*n*
Snow Depth [mm]	Plateau	-76.1	-31.8	117.4	45.2	43,835
	Bog	39.4	20.3	100.8	47.9	54,693
SWE [mm]	Plateau	2.0	1.7	18.2	40.4	6
	Bog	30.8	23.5	37.1	154.9	7
ET [mm/hr]	Landscape	0.012	10.1	0.058	73.7	3,063
	Bog	0.067	47.9	0.089	89.2	1,671
Water Level [mm]	Bog	21.3	71.4	50.2	75.4	16,060

Table III. Definition of evaluation statistics.

Variable	Equation
Mean error	$me = \frac{1}{N}\sum_{i=1}^{N}(S_i - O_i)$
Percent bias	$pbias = 100\frac{\sum_{i=1}^{N}(S_i - O_i)}{\sum_{i=1}^{N} O_i}$
Root mean square error	$rmse = \sqrt{\frac{1}{N}\sum_{i=1}^{N}(S_i - O_i)^2}$
Normalized root mean square error	$nrmse = 100\frac{\sqrt{\frac{1}{N}\sum_{i=1}^{N}(S_i - O_i)^2}}{nval}$ $nval = \begin{cases} sd(O_i) & ,\text{norm} = \text{"sd"} \\ O_{max} - O_{min} & ,\text{norm} = \text{"maxmin"} \end{cases}$
Nash-Sutcliffe efficiency	$nse = 1 - \frac{\sum_{i=1}^{N}(S_i - O_i)^2}{\sum_{i=1}^{N}(O_i - \bar{O})^2}$

2.5 RESULTS

2.5.1 Water Balance

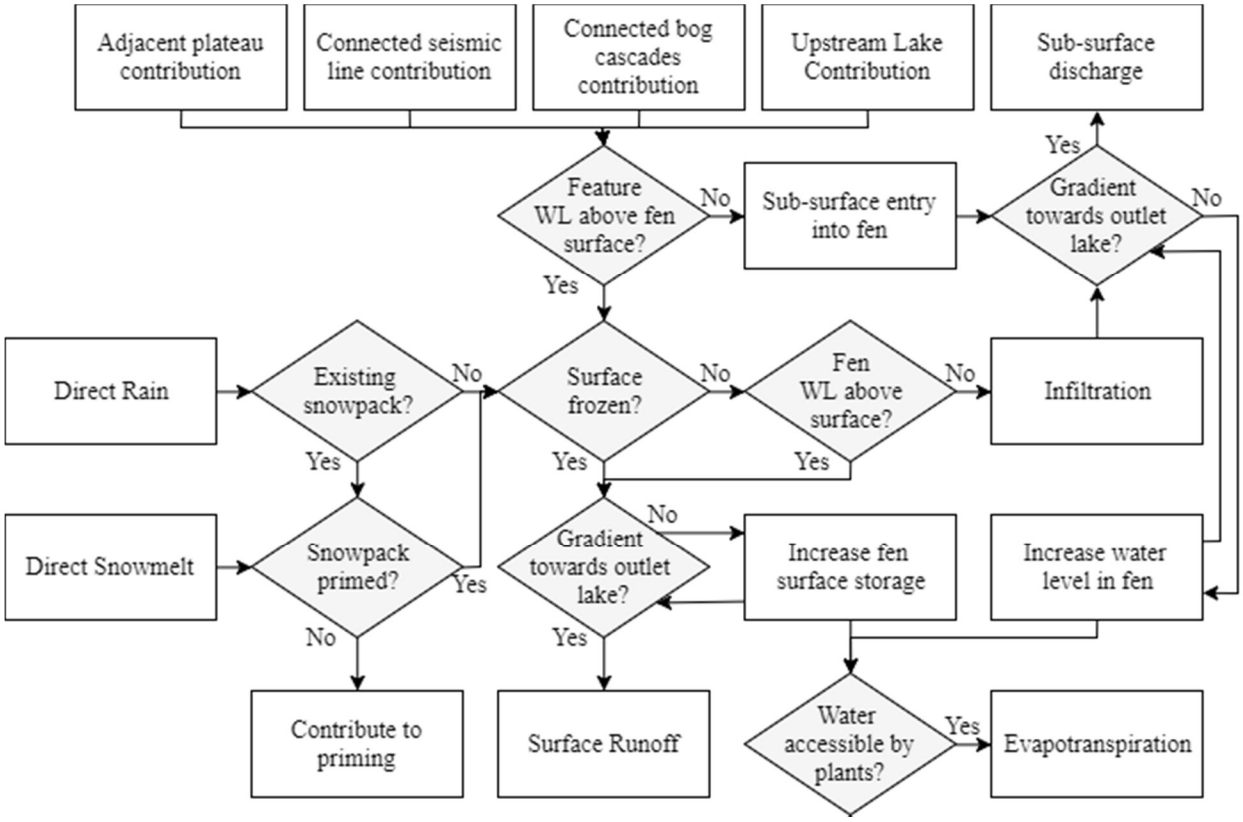

Figure 2. Conceptual diagram of water movement through channel fens in wetland dominated peat rich basins in the discontinuous permafrost zone as determined through field work conducted at the Scotty Creek Research Basin. Rectangles represent processes while diamonds represent yes/no questions. WL: Water Level. Note, bog cascades, seismic lines and lakes may become hydrologically disconnected from a channel fen under sufficiently low water level conditions.

As a result of the fieldwork conducted on the channel fen outlined in Figure 1c, a conceptual model of how water moves through the fen was developed (Figure 2). The channel fen had highest rates of surface runoff during the spring freshet. A layer of seasonal frost at the fen surface was observed during field studies, which may have limited or prevented infiltration of snowmelt water. According to the water balance calculations, 58% of annual surface runoff from the fen occurred during the "spring" snowmelt period between 04/04/2015 and 31/05/2015 (Figure 3b), which accounted for more than 95% of total discharge during the same time period. The water

table reached an average maximum of 23 cm above the ground surface of the fen, and dropped to within 5 cm by 01/06/2015 midway between the lakes, though an area directly next to First Lake remained ponded to a minimum depth of 12 cm above the fen surface during the entire study. During the "summer" period the water table remained consistently near the fen surface and responded quickly to rain events. ET_{fen} exceeded precipitation inputs over this period with an ET_{fen}/rainfall ratio of 1.2 for the summer of 2015 (Figure 3a, 3c). The connected land cover types (surrounding peat plateau, connected bog cascades, and the upstream lake) consistently contributed to the fen and maintained a sufficiently high water level to allow high rates of evaporation and transpiration from the vascular plants. As ET_{fen} rates decreased in the "fall' period, the change in storage in the fen became positive and subsurface discharge peaked. During the "fall" period, between 02/09/2014 and 17/12/2014, the fen subsurface discharge accounted for 45% of total subsurface discharge that occurred during the whole water balance period, 02/09/2014 to 26/08/2015 (Figure 3d). Discharge during the winter was limited to the subsurface, as the surface of the fen remained frozen until after the spring freshet with a maximum measured refreezing depth of 24 cm. Subsurface discharge during the "winter" period accounted for 18% of total annual subsurface discharge. Discharge out of the fen was almost equal to subsurface inputs, with an average positive change in storage of 3 mm/day between 18/12/2014 and 03/04/2015.

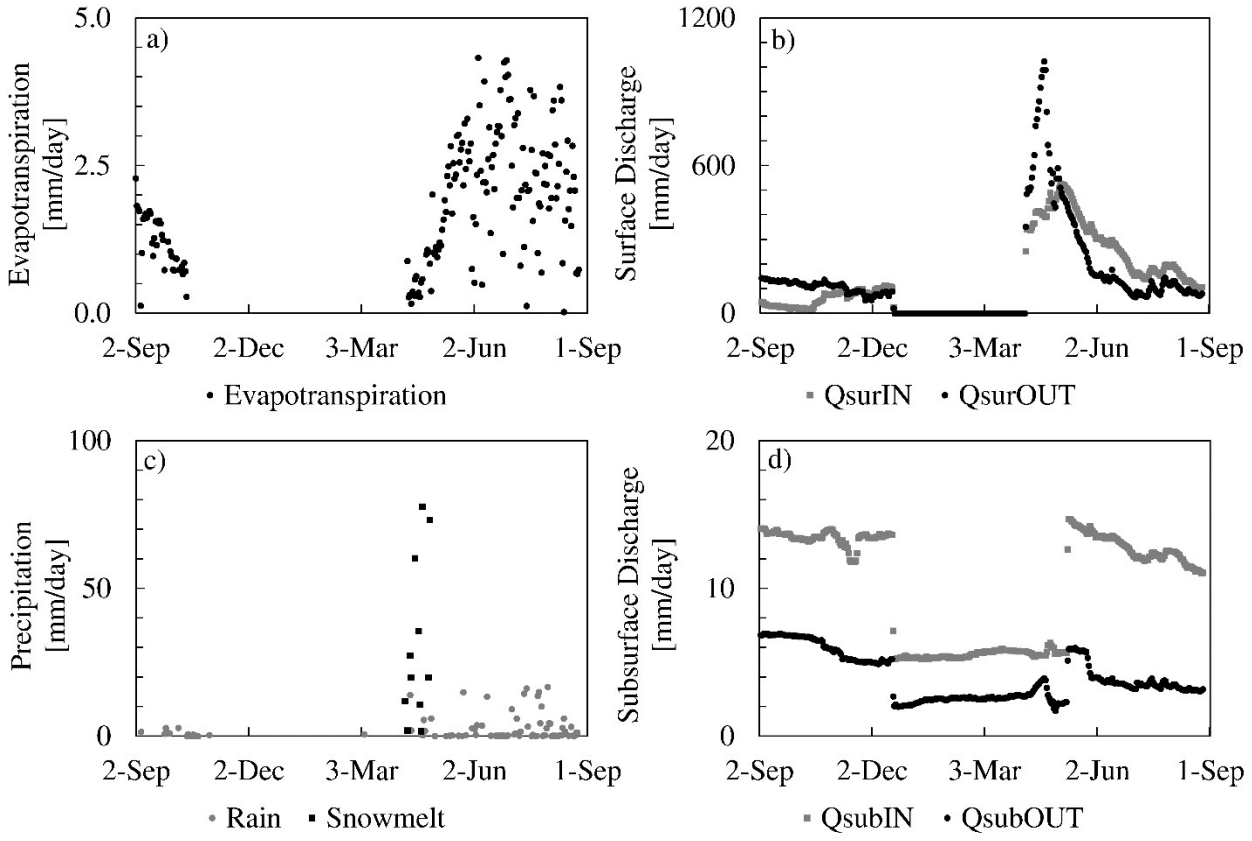

Figure 3. Components of the water balance calculations performed to solve for change in storage, S, in equation 2 for the fall 2014 to fall 2015 time period for (a) evapotranspiration, (b) surface discharge in (QsurIN) and out (QsurOUT) of the channel fen, (c) precipitation inputs as either snowmelt or direct rainfall, and (d) subsurface discharge in (QsubIN) and out (QsubOUT) of the channel fen.

2.5.2 Numerical Model

2.5.2.1 Performance Evaluation

Simulated snow depth was compared to the hourly measured snow depth at points near the peat plateau and bog tripod sites (described above). Simulated SWE was compared to measured SWE from annual snow surveys taken along transects that intersected the bog and peat plateau tripod locations. Snow depth and density were measured at sampling points along the transects to determine SWE, and measured SWE for bog and peat plateau were calculated from averaged

values for all points on the corresponding transects. Modelled snow depth, water level, and evapotranspiration were compared against measurements whose collection is as described above.

The CRHM model output is a depth of water that is stored in the soil column. This depth of water was used to estimate the depth of water table above or below the ground surface using the following assumptions: (1) there is a small amount of water that cannot be drained as it is part of the non-active porosity equal to 0.18 volumetric soil water content (Zhang et al., 2010); (2) all water between the ground surface and the saturated water table is held at this minimum saturation level; (3) all pore space below the water table is saturated with water; and (4) the water table is above the ground when the modelled depression storage (S_d) is larger than 0 mm. The depth to water table is considered positive when below ground, and negative when above ground.

The model successfully captures the variation in hourly measured snow depth in the peat plateau and bog with high (>0.85) r-squared values (Figure 4a, 4b). Though there is an underestimation bias in the peat plateau and an overestimation bias in the bog (Table 2, Figure 4a, 4b), the high *nse* values (Figure 4c, 4d) and small *rmse* values (Table 2) for the simulation period suggest generally good model performance.

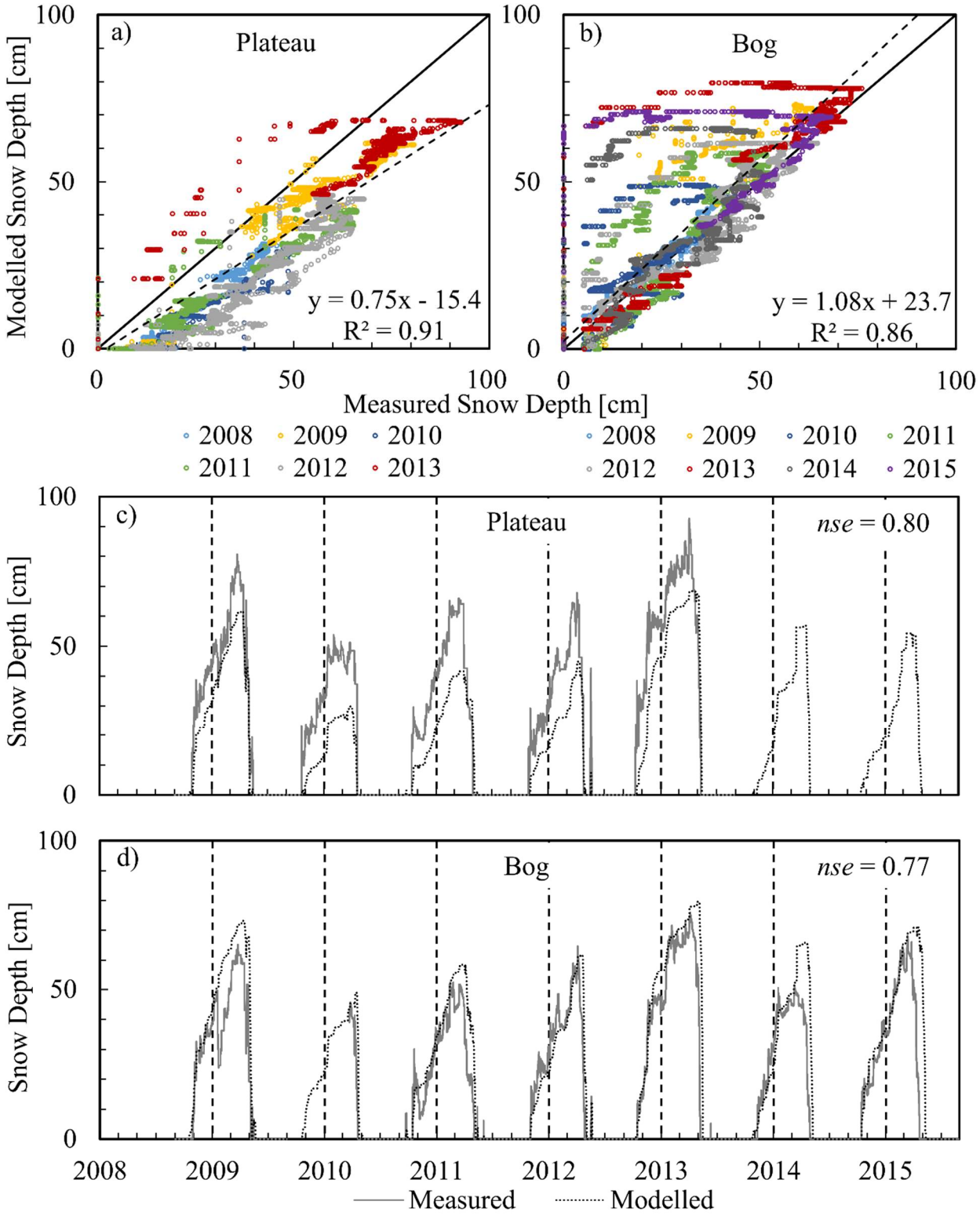

Figure 4. One-to-one plots of (a) plateau and (b) bog snow depth; dashed black lines indicate linear regression for all years and all data points. Time-series data of (c) plateau and (d) bog snow depth. Vertical dashed lines indicate the end of the calendar year.

The model accurately captured the variation in the measured SWE in the peat plateau and bog with r-squared values higher than 0.64 (Figure 5a, 5b). The model was able to capture the end of season SWE for six seasons from 2009 to 2014 for the peat plateau (Figure 5c) with small positive bias and small difference compared to the measurements (Table 2). The model tended to overestimate the end of season SWE for seven seasons from 2009 to 2015 for the bog (Figure 5d), with higher overestimation bias and larger difference compared to the measurements (Table 2). The model's higher overestimation of bog SWE is emphasized by model's overestimation of bog snow density. The average measured density during end-of-season snow surveys conducted in Scotty Creek on the bog land cover type between 2009 and 2015 is 0.17 g/cm^3, the modelled snow density (obtained by dividing the modelled SWE by the modelled snow depth) for the same dates is 0.26 g/cm^3. The model also appears to be underestimating how much snow is sublimated or transported out of the bog HRU, with average difference between total snowfall and measured SWE between 2009 and 2015 of 36 mm and a modelled difference of 4 mm. In the peat plateaus, the model is more accurately capturing annual snow sublimation and transport processes, with a measured difference between snowfall and peat plateau SWE of 40 mm and a modelled difference of 42 mm during the same time period. Wind speeds measured in the bog (Figure 1c) are low and often below the model's threshold required to transport snow.

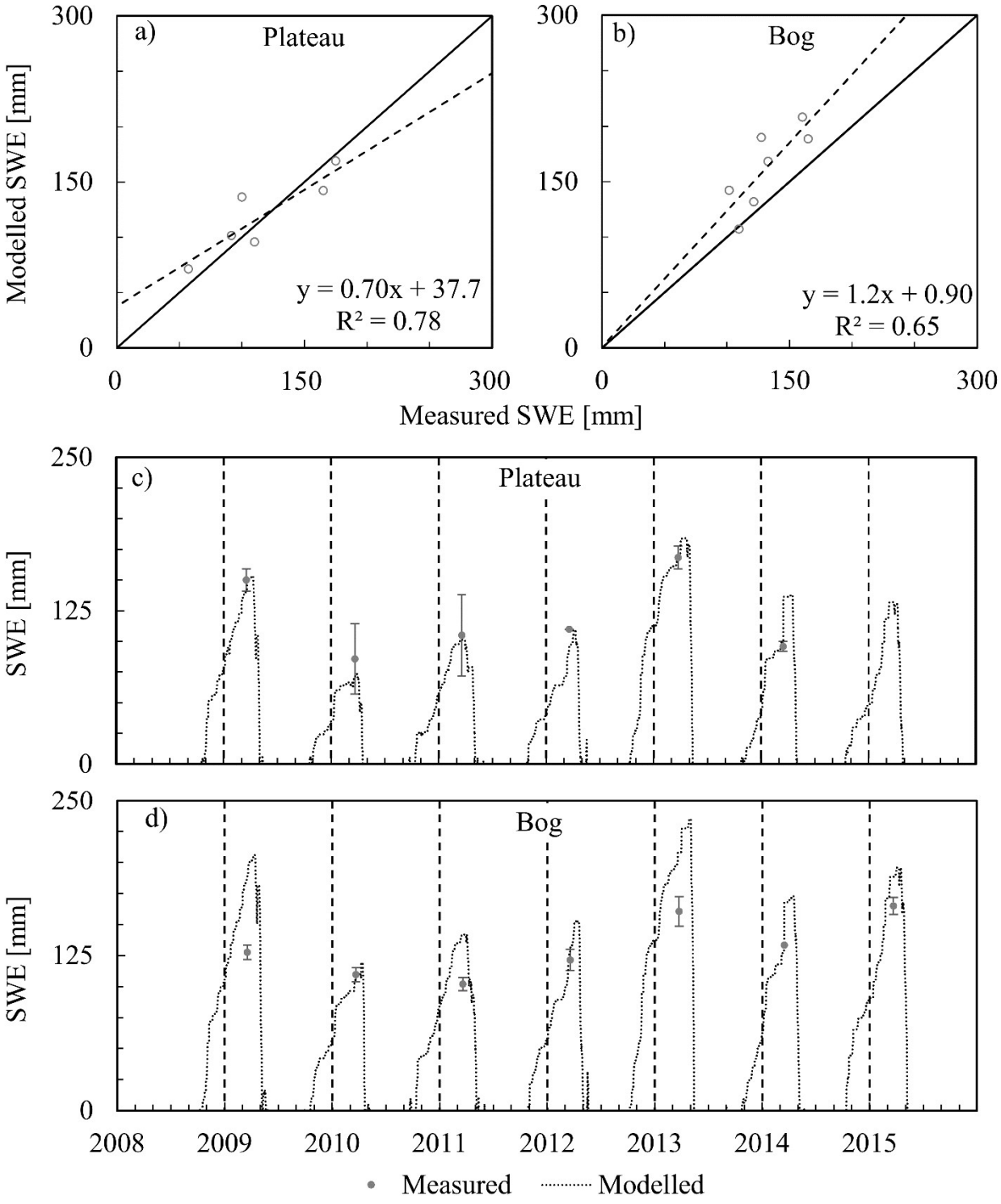

Figure 5. One-to-one plots comparing modelled versus measured values for (a) plateau, and (b) bog snow water equivalent; black dashed lines indicate the linear regression. Time-series data of (c) plateau, and (d) bog snow water equivalent; bars indicate standard error. Vertical dashed lines indicate the end of the calendar year.

At the landscape scale, modelled ET_{land} had a low overestimation bias and relatively small difference compared to the measured ET_{land} (Table 2), but it obtained only 69% of the variation in ET_{land} measurements with low r-squared value (Figure 6a). For the bog HRU, the model captured the majority of the variability of ET_{bog} measurements with a high r-squared value (Figure 6b), though the modelled ET_{bog} showed an overestimation bias and larger differences than for ET_{land} (Table 2). Accurately modelling ET_{bog} is crucial to estimating ET_{land} as wetland ET can significantly exceed peat plateau ET due to higher moisture availability at the surface (Wright et al. 2008). Part of the difference between the model's ability to replicate ET_{bog} versus ET_{land} may be explained by the two approaches used to model peat plateau ET (Penman-Monteith) and ET_{bog} (Preistley-Taylor). Though the Priestly-Taylor method has been shown to accurately predict evaporation from peatlands with non-vascular coverage in Scotty Creek (Connon et al 2015), peatlands with vascular plant cover are better represented by methods that account for atmospheric water vapor conditions in addition to net-radiation such as the Penman-Monteith method (Lafleur & Roulet, 1992). The high availability of input data, including information on the surface conductance of black spruce trees (Zha et al., 2010) allowed for the application of the Penman-Monteith method to simulate ET of the peat plateaus with a high coverage of vascular plants (Quinton et al., 2003). However, tree density on the peat plateaus of Scotty Creek is sufficiently low (Chasmer et al., 2011) to allow for significant contributions from the understory to peat plateau ET (Warren et al., 2017). As the conductance parameter used to calculate ET on peat plateau was based on studies on black spruce trees, it is possible that the model's inability to capture the variability in ET_{land} could be explained by the under-representation of understory conductance on peat plateaus.

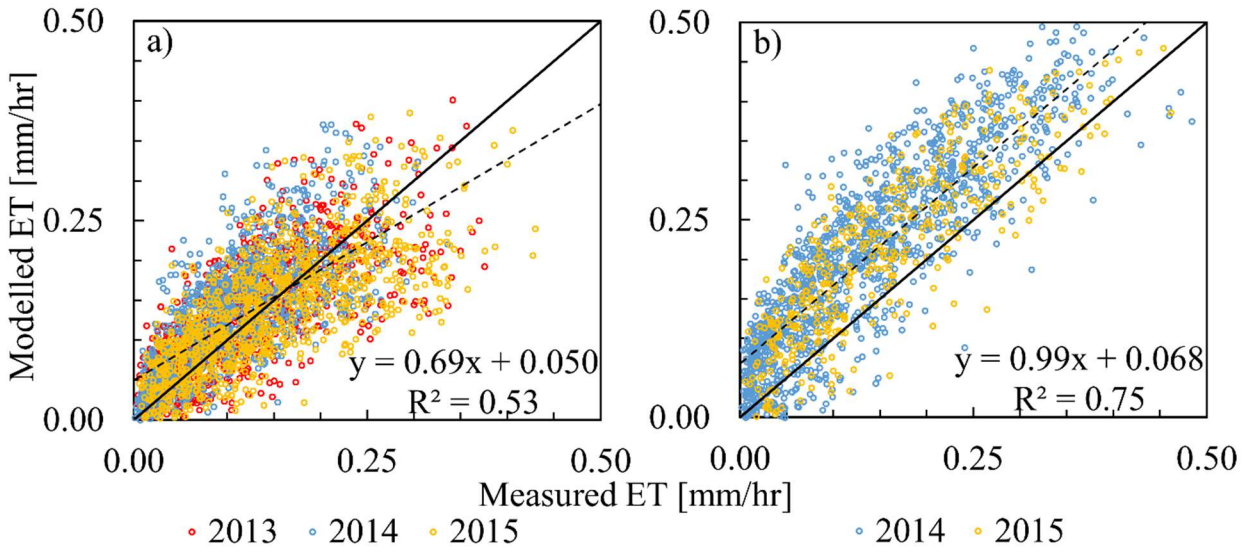

Figure 6. One-to-one graphs comparing modelled versus measured values for (a) landscape, and (b) bog evapotranspiration; dashed black lines indicate the linear regression for all years and all data points.

The model did not accurately simulate water table fluctuations in summers of 2011 and 2014 but adequately captured the bog's water table fluctuations in other years (Figure 7c). On average, there was a 50 mm difference between the modelled and measured bog water table during the simulation period of 2008-2015 (Table 2). Modelled water table's overall overestimation bias (Table 2) was attributed to water table being simluated deeper than the measurements for summers of 2011, 2012, 2013, and 2014. The model output, S_d, used in this performance evaluation for water table depth above the vegetated surface is a proxy. In the model the output S_d operates as a surface storage parameter, and receives inputs not only from excess water in the underlying soil column, but also receives precipitation inputs and runoff from upstream HRUs. This could explain some of the model's lack of skill for simulating above ground storage, for example during the end of summer season of 2011 when the water table was near the surface and large late summer rain storms provided additional inputs.

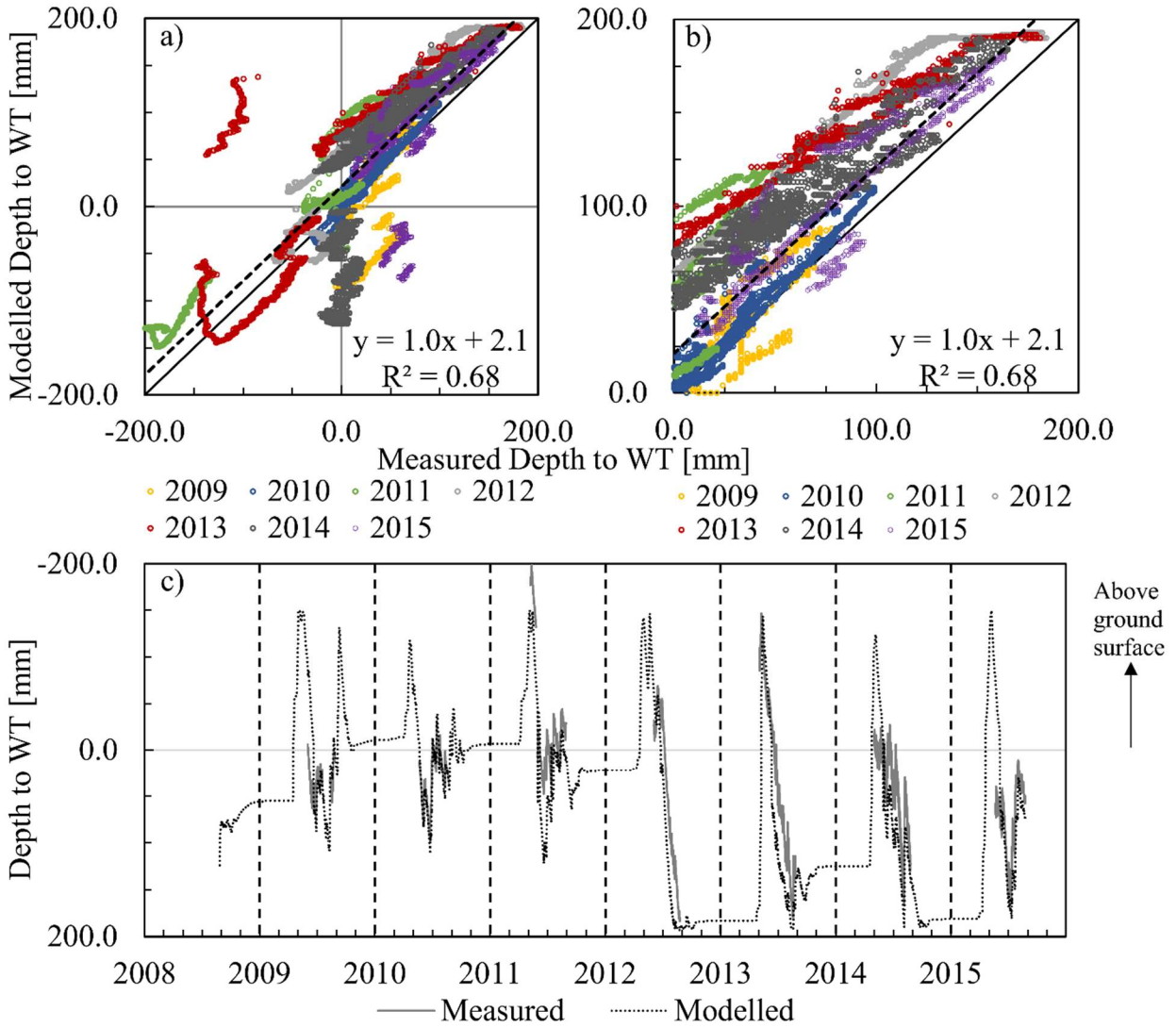

Figure 7. (a) One-to-one graph comparing modelled versus measured water table values for above and below ground, (b) for below ground values only; dashed black lines represent the linear regression for all years and all data points. (c) Time-series of modelled and measured water table values. Vertical dashed lines indicate the end of the calendar year.

2.5.2.2 Sensitivity Analysis

After evaluating the model performance, a sensitivity analysis was conducted to assess the impact of permafrost loss compared to the 2010 permafrost extent on channel fen surface and subsurface flows by varying the ratio of wetland to peat plateau in the modelled sub-basin. When peat plateau is lost in Scotty Creek, it is not possible to predict what type of wetland will replace

the lost forested area, either as bog or channel fen. To account for this uncertainty in the sensitivity analysis, four scenarios of increased wetland area were defined: (1) the simulated peat plateau-reduced area is replaced by expanded bog area (Scenario "All Bog"); (2) the ratio of channel fen–to-bog area of the 2010 HRU delineation in the modelled sub-basin is maintained, with expanded wetland area added at a ratio of 1.6:1 fen to bog (Scenario "Sub-Basin"); (3) the ratio of fen-to-bog area of the greater Scotty Creek watershed is used to determine the ratio at which simulated lost peat plateau area is replaced, with expanded wetland area added at a ratio of 1.9:1 fen to bog (Scenario "Scotty"); (4) all simulated peat plateau reduced area is replaced by expanded fen area (Scenario "All Fen"). All four scenarios were modelled for 10%, 25% and 50% permafrost reductions compared to the 2010 permafrost extent.

Average annual runoff to precipitation ratios between 2009 and 2015 were calculated as the total discharge from the fen HRU divided by the precipitation as recorded by the Geonor after wind under-catch correction. Runoff ratios were also calculated for a "snowmelt" period, defined as the time from the first modelled SWE loss after maximum SWE to the last day snow cover was present in any HRU, and a "summer" period, defined as the time between the first day after all SWE is melted and September 30th of every year.

For all four scenarios, and for all prescribed increments of permafrost loss, the total annual discharge from the fen HRU decreases (Figure 8). On average over the whole modelling period of 2009 to 2015, for every 10% of peat plateau area replaced with wetland area there is a decrease in total annual discharge from the channel fen by 2.5%. Scenario All Bog, the scenario where the simulated reduction of peat-plateau permafrost is replaced entirely with an increase in bog area and no new fen area is modelled, results in the smallest decrease in fen discharge. Scenario All Fen, where lost peat plateau permafrost area is replaced with fen area and no new bog area is

modelled, results in the largest decrease in fen discharge. The impacts of permafrost reduction on the annual discharge volume were variable from year to year depending on wet or dry conditions. The decrease in discharge from the fen HRU was greater in wet years, where discharge from the modelled sub-basin is larger than 220 mm/yr, than in dry years. For instance, for the 50% permafrost reduction in Scenario Sub-Basin, annual cumulative discharge decreased by 53 mm (345 mm to 292 mm) in 2009 when water year precipitation was 598 mm but dropped by only 19 mm (168 mm to 149 mm) in 2013 when the water year precipitation of 348 mm was much less (Figure 8d).

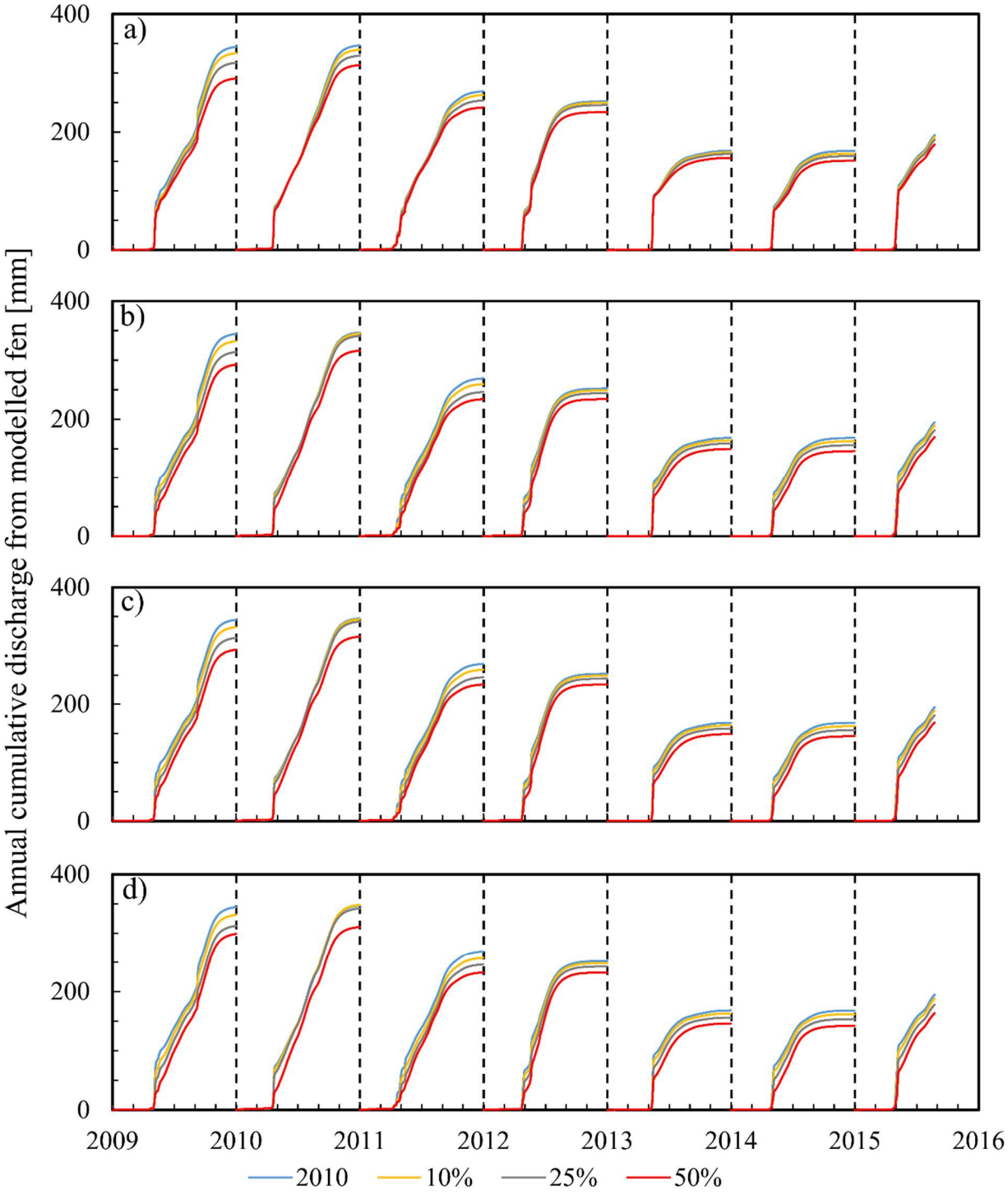

Figure 8. Annual cumulative discharge from Fen HRU for the modelled subarctic muskeg watershed for 10%, 25% and 50% modelled permafrost loss compared to the 2010 permafrost extent for (a) Scenario All Bog; (b) Scenario Sub-Basin; (c) Scenario Scotty; and (d) Scenario All Fen. Vertical dashed lines indicate the end of the calendar year.

Though the annual discharge from the fen HRU decreased in all scenarios, this does not hold true on the seasonal basis. Scenario Sub-Basin is used to illustrate this pattern (Figure 9b). During large late summer storms, identified as storms greater than 25 mm/d, and during snowmelt the modelled hourly discharge from the fen HRU is up to 75% lower when compared to the 2010 permafrost extent modelled discharge. Because the decrease coincides with the large peak in the channel fen hydrograph (Figure 9a, c), this results in a significant decrease in total annual discharge. During low-flow periods just before the snow freshet begins and for extended periods in the summer the hourly discharge from the fen HRU is greater than the 2010 modelled fen HRU discharge. To investigate this further, the total discharge from the fen HRU was separated into its three modelled layers; groundwater discharge (25 cm – 400 cm below surface), vadose zone discharge (0 cm – 25 cm below surface), and surface runoff.

Scenario Sub-Basin is used to illustrate the change in discharge from the three modelled layers (Figure 10). The modelled increase in groundwater discharge compared to the 2010 permafrost extent was most pronounced during low flow periods (e.g. August to December), and the annual cumulative difference was greatest in dry years (e.g. 2013 and 2014) with a total discharge of less than 220 mm/yr (Figure 10a). The increased vadose zone (0 cm – 25 m layer) discharge is more prominent in wet years (e.g. 2009 and 2010, Figure 10b). Surface runoff discharge was most sensitive to permafrost reductions (Figure 10c). For the 50% permafrost loss, reductions in surface runoff ranged from 48% in a wet year (i.e. 2009) to 27% in a dry year (i.e. 2013). Though the discharge in both 0 mm – 25 cm and 25 cm– 400 cm layers increased with modelled permafrost loss, a reduction in surface runoff was not compensated for, resulting in an overall reduction in total discharge from the fen HRU in all scenarios and for all amounts of simulated permafrost loss.

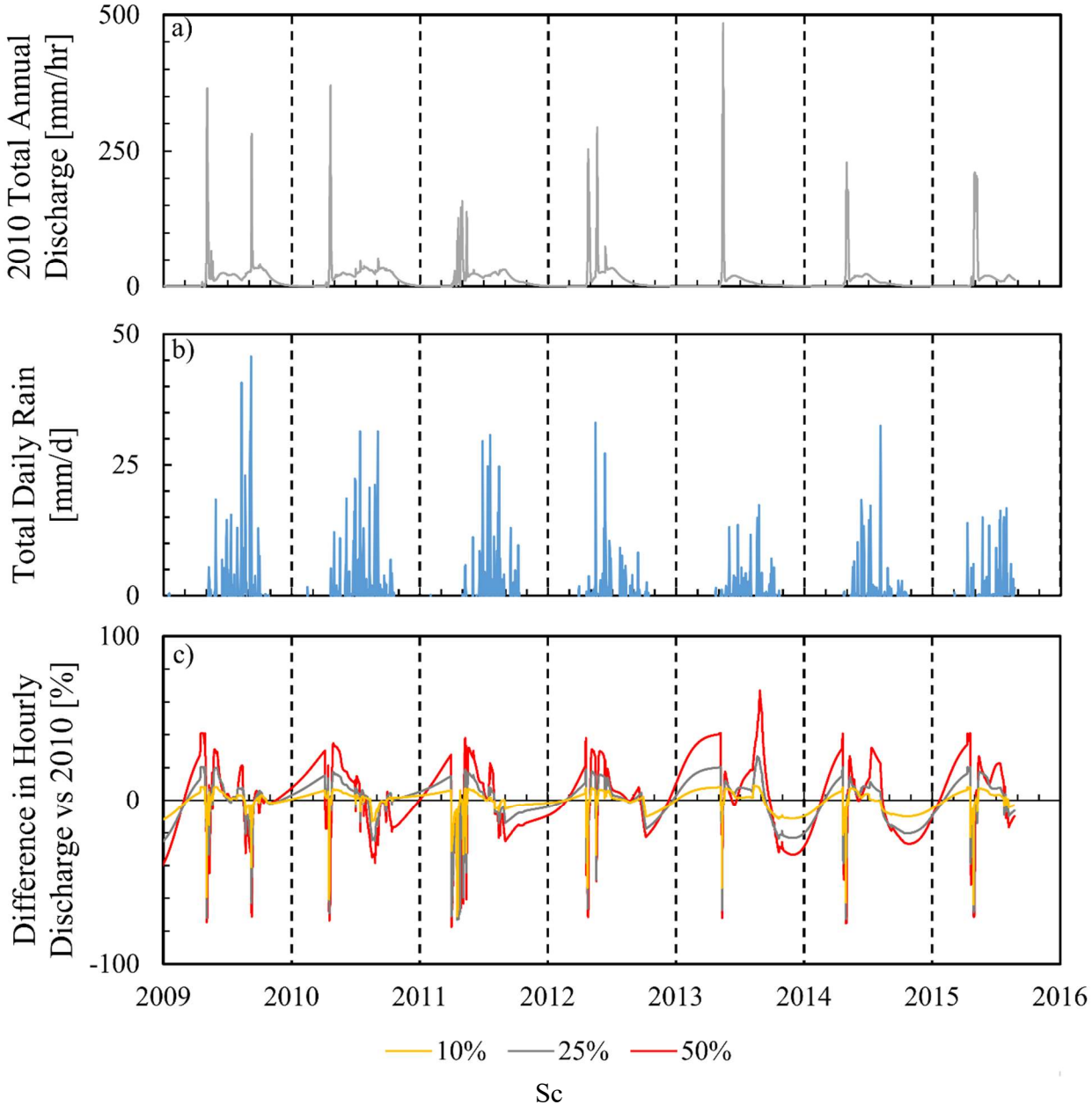

Figure 9. (a) Total annual discharge out of the channel fen sub-basin with no simulated reduction in permafrost extent; (b) Daily total rainfall in the Fen HRU; and (c) Percent difference between the hourly discharge from the Fen HRU comparing the Scenario Sub-Basin and the 2010 model run for simulated 10%, 25% and 50% reduction in permafrost extent. Vertical dashed lines indicate the end of the calendar year.

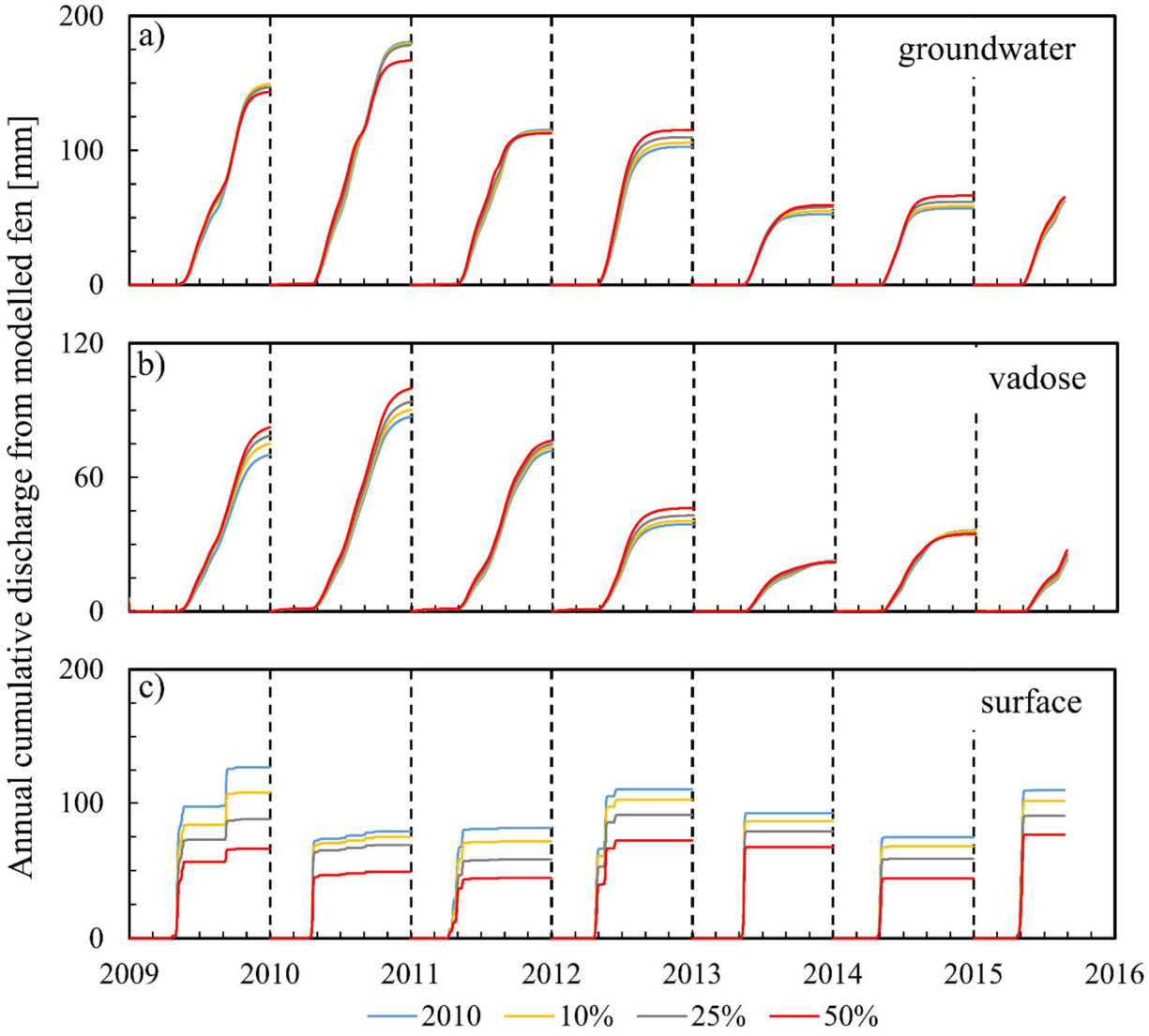

Figure 10. Annual cumulative discharge from the Fen HRU for the modelled subarctic muskeg watershed from the (a) groundwater zone (25 m - 400 cm below fen surface); (b) vadose zone (0 cm - 25 cm below fen surface); and (c) surface runoff for Scenario Sub-Basin for the 2010 model run and for 10%, 25% and 50% reduction in permafrost extent. Vertical dashed lines indicate the end of the calendar year.

2.6 DISCUSSION

Water balance calculations suggest that the channel fen is dominated by surface runoff (Figure 3b). It is therefore crucial for numerical modelling to accurately predict water table position and snowmelt rates for channel fens. These findings suggest that as permafrost continues to thaw, annual discharge will decrease, with the greatest decreases from surface flows. The

discharge from the fen also shows decreased intra-annual variability. Simulated discharge is higher during periods of low-flow, and peak flows during late summer storms and during the spring freshet are lower as permafrost thaws. This pattern of increased minimum discharge and decreased maximum discharge has been shown to be a common pattern in basins undergoing permafrost degradation (Frampton et al., 2013). Some mechanisms that may explain these changes in wetland discharge include increases in basin ET and in storage.

Table IV. Average Annual Total Evapotranspiration over the Sub-Basin.

Scenario	Lake	Bog	Fen	Plateau	Sub-Basin ET [mm/km^2]
	Percent of Land Cover [%]				
Average ET [mm/km^2]	156	384	388	92	
2010 Permafrost Extent	44	12	19	25	210
Scenario Sub-Basin 10%	44	13	20	23	218
Scenario Sub-Basin 25%	44	14	23	19	229
Scenario Sub-Basin 50%	44	16	27	13	247

In the sensitivity analysis, the average annual total ET per unit area for any HRU is not changed, only relative HRU areas (Table 4). Over the basin, annual ET from bogs and channel fens is higher than from the forested peat plateau, with CRHM simulated values of 384 mm, 388 mm and 92 mm, respectively. The sensitivity analysis shows that as the peat plateau shrinks and wetland areas expand with permafrost degradation, the overall watershed ET flux increases, as also reported by Helbig et al. (2016). ET rates increase by approximately 3.5%, or the equivalent of 7.4 mm/km^2 annually, for every 10% decrease in permafrost area compared to the 2010 extent. As ET is a major source of water loss in bogs (Connon et al., 2014) and at the basin scale accounts for between 65% and 70% of total incoming precipitation between 1999 and 2002 (Quinton & Hayashi, 2008), an increase in evapotranspirative loss at the basin scale could explain the reduction in events where the water table surpasses the surface and contributes to reduced annual runoff.

Unlike peat plateaus, the bogs and fens in the sub-basin were parameterized to store water above the ground in topographic depressions. Therefore, when the modelled peat plateau area is reduced, the area occupied by bogs and fens, collectively the wetland area, is proportionately increased. Consequently, the fraction of the landscape with a depression storage capacity is increased. This landscape fraction functions as a hydrological buffer separating the runoff producing areas (*i.e.* peat plateaus) from the basin drainage network of channel fens. Permafrost thaw induced widening of this buffer increases the flow length and travel time through it, and as a result, the hydraulic response of channel fens is expected to be increasingly attenuated with on-going permafrost thaw. A widening wetland buffer will also lower the elevation of the wetland water table since the hydrological input (*e.g.* snowmelt water) is distributed over a larger area. As a result, greater hydrological input would be needed to overcome the depression storage capacity so that overland flow could occur.

The reduction in peak discharge and increased low flows is apparent when calculating runoff ratios based on simulated discharge. The average annual runoff ratio for the seven-year period 2009-2015 was 0.54, assuming a constant areal permafrost extent equal to the extent in 2010. Reducing the permafrost coverage by 50%, lowered the runoff ratio to 0.48, highlighting the modelled sub-basin's reduction in efficiency at exporting atmospheric inputs. This change is most evident during the "snowmelt" period, where average snowmelt runoff ratios declined from 0.47 based on the 2010 permafrost extent to 0.31 assuming a 50% reduction of permafrost extent. The "summer" period did not show this behavior. Average summer runoff ratios remained constant at 0.58 due to small increases in groundwater and vadose zone discharge during the higher low-flow periods.

Though recent studies (e.g. Connon et al., 2014) have highlighted increased hydrological connectivity as a mechanism behind increases in discharge and runoff ratios for Scotty Creek for the period 1995-2011, it is important to note that the present study assumed that all areas in the model domain were hydrologically-connected to the channel fen and to the basin outlet. This is a critical distinction to make since Connon et al. (2014) argue that permafrost thaw is increasing the hydrological connectivity of the landscape to the basin outlet, a process that could account for rising stream flows in the absence of rising precipitation. The modelled sub-basin does not represent changes in contributing area and the potential effects of bog capture; contributing area is instead held constant at its highest possible value and the composition of that area is changed with the goal of predicting changes in discharge in this sub-basin once further bog capture is no longer possible. Therefore, previous literature highlighting the mechanisms behind increasing discharge tied to shrinking permafrost areas do not contradict the findings of this study.

This study also does not address issues of changing climate directly in the form changes to temperature or precipitation inputs, only the sensitivity of the system under current climate conditions to further land cover change. However, forecasted increases in mean annual air temperature and decreases in end of season SWE (IPCC 2014) would interact simultaneously with land cover change to impact peatland discharge. Increased air temperature could act as a positive feedback to further the decrease in discharge projected by this study if increasing air temperature results in increased evapotranspiration (Tarnocai, 2006). Decreased end of season SWE in this basin could compound with the effects of changing land cover highlighted in this study. By simultaneously decreasing the volume of snowmelt added to the system while increasing the area of the system capable of storing ponded water the depth of water above the surface in bogs and

fens is further reduced, potentially resulting in an even larger decrease in channel fen discharge during peak flow.

2.7 CONCLUSION

Based on application of a CRHM model, reductions in permafrost extent are predicted to decrease total annual discharge in a channel fen in the Scotty Creek watershed due to increased surface storage capacity, reduced runoff efficiency, and increased basin scale evapotranspiration. On average, there is a 2.5% reduction in total annual discharge from the modelled channel fen for every 10% loss of peat plateau area in the sub-basin. In general, as wetland area increases, the peak discharge during the snowmelt season and during large late-summer storms decreases. The discharge during periods of low discharge slightly increases as wetland area increases. Both the total annual groundwater and vadose zone discharge increase slightly, showing a change in flow pathways as permafrost decays and peat plateau is replaced by wetland. However, the reduction of total annual runoff dominates, resulting in an overall decrease in total annual discharge as peat plateau and permafrost area decrease. The current trend of increasing discharge observed in the Scotty Creek basin may not be permanent, as this model shows that a completely connected sub-basin results in decreasing channel fen discharge with further land cover change.

3. CONCLUSION

3.1 Principal Findings

As permafrost extent was incrementally reduced, model scenarios showed that total annual discharge from the channel fen sub-basin reduced; for every 10% prescribed loss of permafrost extent compared to the 2010 scenario discharge decreased by 2.5%, depending on the ratio of bog to channel fen areas. The decrease in total annual discharge was not reflected in all components of total discharge. Total annual discharge from the vadose zone (0 cm below fen surface to 25 cm) and groundwater zone (25 cm below fen surface to 400 cm) increased in all modelled years. However, the reduction in total annual runoff was significantly large in order to compensate for the increase in below ground reduction for an overall reduction in wetland total annual discharge. The model also showed a reduction in intra-annual variability, with lower peak discharges during the spring freshet and larger discharges during low-flow seasons.

These changes may be explained through two mechanisms. First, an increase in basin ET, and second, an increase in basin storage. Although the total ET modelled in the individual HRU types did not change with the prescribed reductions in permafrost extent, the difference in total annual ET between HRU types is sufficiently high that the combined basin-scale ET rate increases as wetland area increases and peat plateau area decreases. Therefore, this modelling application shows that as permafrost extent is incrementally reduced, basin scale evapotranspiration increases; for every 10% prescribed loss of permafrost extent compared to the 2010 scenario basin evapotranspiration increases by 3.5%. Unlike peat plateaus, wetland areas are capable of storing water at the surface in ponded depressions; changing the proportional cover of wetlands in the modeled sub-basin results in an increased basin wide capacity to store water. Increasing wetland area therefore increases the buffering zone between runoff generating areas (*i.e.* peat plateaus) and

the basin drainage network, acting to attenuate peak flows and maintain subsurface discharge in low flow periods.

The Scotty Creek watershed has historically been experiencing an increase in total annual discharge. Field studies on the changing hydrology of the region have identified potential sources for this increase in basin discharge, including the strong influence of expanding wetland areas in the form of bog capture and bog cascades. This study aims to understand a system where the mechanisms of bog capture can no longer increase basin contributing area (*i.e.* is when all portions of the landscape contribute to basin discharge), and predicts a reversal in the current trend in total annual discharge.

3.2 Future Work

The development of a conceptual model outlining the movement of water through channel fens, and the incorporation of this with an extensive body of previous work to build and parameterize a numerical model presents a significant body of work contributing to our ability to adapt research into physical processes at Scotty Creek into large scale hydrological modelling. The modelled bog-fen-plateau complex represents an example of the typical wetland-forest system representative of the headwaters of Scotty Creek, providing a foundation for which further modelling efforts could build on. To expand the modelling work undertaken as part of this thesis, future work must take into account the presence of mineral uplands that are more prominent in the lower one-third of the basin (Chasmer et al., 2014). Modelling of mineral uplands may require further fieldwork, as they are conventionally understood to lack permafrost below their surface, and as such may not be able to be approximated by our hydrological understanding of peat plateaus. Parameters such as porosity, rooting depth, hydraulic conductivity, and vegetation characteristics, as well as spatial analysis of slope, aspect and elevation would be required before

this land cover type could be incorporated in future modelling in CRHM if the modules used in the modelling work of this thesis are used. Under the permafrost conditions of 2017, not all bogs are directly connected to a channel fen (Chasmer et al., 2014; Connon et al., 2015). In order to scale up this modelling project from an individual fen-bog-plateau complex to a larger representative area, work would be required to incorporate seasonally connected bogs as part of a bog cascades, as well as a conceptualization of how bogs connect in a cascade (i.e., number of bogs typically in a chain, number of bogs that contribute to a downstream bog, etc) to establish HRU number and sequence.

This model structure could also be used to assess the impact of currently observed and future projects of climate change. Further increases in air temperature (IPCC 2014), and decreases in end of season SWE (IPCC 2014) would all interact simultaneously with land cover change to impact peatland discharge. Increasing air temperature could act as a positive feedback to further the decrease in discharge projected by this study if increasing air temperature results in increased evapotranspiration or accelerated permafrost thaw. Decreased end of season SWE in this basin could compound with the effects of changing land cover highlighted in this study. By simultaneously decreasing the volume of snowmelt added to the system while increasing the area of the system capable of storing ponded water the depth of water above the surface in bogs and fens is further reduced, potentially resulting in an even larger decrease in channel fen discharge during peak flow. The simultaneous interactions of multiple impacts of climate change could be assessed using CRHM for the Scotty Creek basin as a whole, or for a smaller sub-basin in a similar fashion to this body of work.

4. REFERENCES

Alexeev, G. A., Kaljuzhny, I. L., Kulik, V. Y., Pavlova, K. K., & Romanov, V. V. (1972). Infiltration of snowmelt water into frozen soil. *The role of snow and ice in hydrology, Symposia*, (pp. 313-325). Banff, Canada.

Ayers, H. D. (1959). Influence of soil profile and vegetation characteristics on net rainfall supply to runoff. *Proceedings of Hydrology Symposium, 1*, 198-205.

Aylsworth, J. M., Burgess, M. M., Desrochers, D. T., Duk-Rodkin, A., Robertson, T., & Traynor, J. A. (2000). Surficial geology, subsurface materials, and thaw sensitivity of sediments. In *The physical environment of the Mackenzie Valley, Northwest Territories: a base line for the assessment of environmental change* (pp. 41-48). Geological Survey of Canada Bulletin.

Baltzer, J. L., Veness, T., Chasmer, L. E., Sniderhan, A. E., & Quinton, W. (2014). Forests in thawing permafrost: fragmentation, edge effects, and net forest loss. *Global Change Biology, 58*(247), 824-834.

Belyea, L. R., & Clymo, R. S. (2001). Feedback control of the rate of peat formation. *Proceedings of the Royal Society of London B: Biological Sciences, 268*(1473), 1315-1321.

Braverman, M., & Quinton, W. L. (2016). Hydrological impacts of seismic lines in the wetland-dominated zone of thawing, discontinuous permafrost, Northwest Territories, Canada. *Hydrological Processes, 30*(15), 2617-2627.

Brown, J. E., & Williams, G. P. (1972). *The freezing of peatland.* Ottawa: National Research Council of Canada Division of Building Research.

Brunt, D. (1932). Notes on radiation in the atmosphere. *Quaterly Journal of the Royal Meteorological Society, 7*(3), 358-420.

Bullock, A., & Acreman, M. (2003). The role of wetlands in the hydrological cycle. *Hydrology and Earth Sciences Discussions*, 358-389.

Burgess, M. M., & Smith, S. L. (2000). Shallow ground temperatures. In *The physical environment of the Mackenzie Valley, Northwest Territories: a base line ofr the assessment of environmental change* (pp. 89-103). Geological Survey of Canada Bulletin.

Camill, P. (2005). Permafrost thaw accelerates in boreal peatlands during late-20th century climate warming. *Climatic Change, 68*(1), 135-152.

Changwei, X., & gough, W. A. (2013). A simple thaw-freeze algorithm for a multi-layered soil using the Stefan equation. *Permafrost and Periglacial Processes, 24*(3), 252-260.

Chasmer, L., Hopkinson, C., & Quinton, W. (2010). Quantifying errors in discontinuous permafrost plateau change from optical data, Northwest Territories, Canada. *Canadian Journal of Remote Sensing, 36*(S2), S211-S223.

Chasmer, L., Quinton, W. L., Hopkinson, C., Petrone, R., & Whittington, P. (2011). Vegetation canopy and radiation controls on permafrost plateau evolution within the discontinuous permafrost zone, Northwest Territories, Canada. *Permafrost and Periglacial Processes, 22*(3), 199-213.

Chasmer, L., Veness, T., Quinton, W., & Baltzer, J. (2014). A decision-tree classification for low-lying complex land cover types within the zone of discontinuous permafrost. *Remote Sensing of Environment, 143*, 73-84.

Chow, V. T. (1959). *Open channel hydraulics.* New York: McGraw-Hill Book Company, Inc.

Chow, V. T. (1964). *Handbook of Applied Hydrology.* New York: McGraw-Hill Book Company, Inc.

Christensen, B. (2014). Unpublished Master's Thesis. *Permafrost development and active-layer hydrology of peat plateaus in wetland-dominated*. Calgary, AB, Canada: University of Calgary.

Connon, R. F., Quinton, W. L., Craig, J. R., & Hayashi, M. (2014). Changing hydrologic connectivity due to permafrost thaw in the lower Liard River Valley, NWT, Canada. *Hydrological Processes, 28*(14), 4163-4178.

Connon, R. F., Quinton, W. L., Craig, J. R., Hanisch, J., & Sonnentag, O. (2015). The hydrology of interconnected bog complexes in discontinuous permafrost terrains. *Hydrological Processes, 29*(18), 3831-3847.

Cordeiro, M. R., Wilson, H. F., Vanrobaeys, J., Pomeroy, J. W., Fnag, X., & Team, T. R.-A. (2017). Simulating cold-region hydrology in an intensively drained agricultural watershed in Manitoba, Canada, using the Cold Regions Hydrological Model. *Hydrology and Earth System Sciences, 21*(7), 3483-3506.

Cornwall, C., Horiuchi, A., & Lehman, C. (2015). NOAA Solar Calculator. *USA: Department of Commerce*.

Damman, A. W. (1986). Hydrology, development, and biogeochemistry of ombrogenous peat bogs with special reference to nutrient relocation in a western Newfoundland bog. *Canadian Journal of Botany, 64*(2), 384-394.

Dimitrov, D. D., Bhatti, J. S., & Grant, R. F. (2014). The transition zones (ecotone) between boreal forests and peatlands: Ecological controls on ecosystem productivity along a transition zone between upland black spruce forest and a poor forested fen in central Saskatchewan. *Ecological modelling, 291*, 96-108.

Dornes, P. F., Tolson, B. A., Davison, B., Pietroniro, A., Pomeroy, J. W., & Marsh, P. (2008). Regionalisation of land surface hydrological model parameters in subarctic and arctic environments. *Physics and Chemistry of the Earth, 33*, 1081-1089.

Ellis, C. R., Pomeroy, J. W., Brown, T., & MacDonald, J. (2010). Simulation of snow accumulation and melt in needleleaf forest environments. *Hydrology and Earth System Sciences, 14*(6), 925-940.

Environment and Climate Change Canada. (2017). Canadian Climate Normals 1981-2010. *Station Data (Fort Simpson A)*. Retrieved from http://climate.weather.gc.ca/climate_normals/

Fan, S. M., Wofsy, S. C., Bakwin, P. S., Jacob, D. J., & Fitzjarrald, D. R. (1990). Atmosphere-biosphere exchange of CO2 and O3 in the Central Amazon Forest. *Journal of Geophysical Research Letters, 95*, 16851-16864.

Fang, X., & Pomeroy, J. W. (2016). Impact of antecedent conditions on simulations of a flood in a mountain headwater basin. *Hydrological Processes, 30*(16), 2754-2772.

Fang, X., Pomeroy, J. W., Eliis, C. R., MacDonald, M. K., DeBeer, C. M., & Brown, T. (2013). Multi-variable evaluation of hydrological model predictions for a headwater basin in the Canadian Rocky Mountains. *Hydrology and Earth System Sciences, 17*(4), 1635-1659.

Fang, X., Pomeroy, J. W., Westbrook, C. J., Guo, C., Minke, A. G., & Brown, T. (2010). Prediction of snowmelt derived streamflow in a wetland dominated prairie basin. *Hydrology and Earth System Sciences, 14*(6), 991-1006.

Farouki, O. T. (1981). The thermal properties of soils in cold regions. *Cold Regions Science and Technology, 5*(1), 67-75.

Ferone, J. M., & Devito, K. J. (2004). Shallow groundwater-surface water interactions in pond-peatland complexes along a Boreal Plains topographic gradient. *Journal of Hydrology, 292*(1), 75-95.

Frampton, A., Painter, S. L., & Destouni, G. (2013). Permafrost degradation and sub-surface flow changes caused by surface warming trends. *Hydrogeology Journal, 21*(1), 271-280.

Frampton, A., Painter, S., Lyon, S. W., & Destouni, G. (2010). Non-isothermal, three-phase simulations of near-surface flows in a model permafrost system under seasonal variability and climate change. *Journal of Hydrology, 403*(3), 352-359.

Frey, K. E., & McClelland, J. W. (2009). Impacts of permafrost degradation on arctic river biogeochemistry. *Hydrological Processes, 23*(1), 169-182.

Frey, K. E., Siegel, D. I., & Smith, L. (2007). Geochemistry of west Siberian streams and their potential response to permafrost degradation. *Water Resources Research, 43*.

Fritz, C., Campbell, D. I., & Schipper, L. A. (2008). Oscillating peat surface levels in a restiad peatland, New Sealand - magnitude and spatiotemporal variability. *Hydrological Processes, 22*(17), 3264-3274.

Garnier, B. J., & Ohmura, A. (1970). The evaluation of surface variations in solar radiation income. *Solar Energy, 13*(1), 21-34.

Gordon, J., Quinton, W., Branfireun, B. A., & Olefeldt, D. (2016). Mercury and methylmercury biogeochemistry in a thawing permafrost wetland complex, Northwest Territories, Canada. *Hydrological Processes, 30*(20), 3627-3638.

Granger, R. J., & Gray, D. M. (1990). A net radiation model for calculating daily snowmelt in open environments. *Hydrology research, 21*(4-5), 217-234.

Gray, D. M., & Landine, P. G. (1988). An energy-budget snowmelt model for the Canadian Prairies. *Canadian Journal of Earth Sciences, 25*(8), 1292-1303.

Gray, D. M., Landine, P. G., & Granger, R. J. (1984). An infiltration model for frozen Prairie soils. *Canadian Society of Agricultural Engineers, 1984 Annual Meeting.* Winnipeg, Canada.

Hayashi, M., & Quinton, W. L. (2005). [Salt-tracer test for saturated hydraulic conductivity in a channel fen, Scotty Creek]. *Unpublished raw data*.

Hayashi, M., Goeller, N., Quinton, W. L., & Wright, N. (2007). A simple heat-conduction method for simulating the frost-table depth in hydrological models. *Hydrological Processes, 21*(19), 2610-2622.

Hayashi, M., Quinton, W. L., Pietroniro, A., & Gibson, J. J. (2004). Hydrologic functions of wetlands in a discontinuous permafrost basin indicated by isotopic and chemical signatures. *Journal of Hydrology, 296*(1), 81-97.

Helbig, M., Chasmer, L. E., Desai, A. R., Klun, N., Quinton, W. L., & Sonnentag, O. (2017a). Direct and indirect climate change effects on carbon dioxide fluxes in a thawing boreal forest-wetland landscape. *Global Change Biology, 23*, 3231-3248.

Helbig, M., Chasmer, L., Kljun, N., Quinton, W., Treat, C., & Sonnentag, O. (2017b). The positive net radiative greenhouse has forcing of increasing methane emissions from a thawing boreal forest-wetland landscape. *Global Change Biology, 23*(6), 2413-2427.

Helbig, M., Quinton, W. L., & Sonnentag, O. (2017c). Warmer spring conditions increase annual methane emissions from a boreal peat landscape with sporadic permafrost. *Environmental Research Letters, 12*(11).

Helbig, M., Wischnewski, K., Kljun, N., Chasmer, L. E., Quinton, W. L., Detto, M., & Sonnentag, O. (2016). Regional atmospheric cooling and wetting effect of permafrost thaw-induced boreal forest loss. *Global Change Biology, 22*(12), 4048-4066.

Hogan, J. M., Van der Kamp, G., Barbour, S. L., & Schmidt, R. (2006). Field methods for measuring hydraulic properties of peat deposits. *Hydrological Processes, 20*(17), 3635-3649.

Holden, J. (2005). Peatland Hydrology and Carbon Release: Why Small-Scale Process Matters. *Philosophical Transactions of the Royal Society of London: Mathematical, Physical and Engineering Sciences, 363*(1837), 2891-2913.

Ingram, H. A. (1978). Soil layers in mires: function and terminology. *European Journal of Soil Science, 29*(2), 224-227.

IPCC. (2014). Impacts, adaptation, and vulnerability. Part B: Regional aspects. In *Contribution of working group II to the Fifth assessment report of the intergovernmental panel on climate change.* Cambridge, United Kingdom and New York: Cambridge University Press.

Jorgenson, M. T., Racine, C. H., Walters, J. C., & Osterkamp, T. E. (2001). Permafrost degradation and ecological changes associated with a warming climate in central Alaska. *Climatic Change, 48*(4), 551-579.

Kellner, E. (2001). Surface energy fluxes and control of evapotranspiration from a Swedish Sphagnum mire. *Agricultural and Forest Meteorology, 110*(2), 101-123.

Kim, J., & Verma, S. B. (1996). Surface exchange of water vapour between an open Sphagnum fen and the atmosphere. *Boundary-Layer Meteorology, 79*(3), 243-264.

Krogh, S. A., Pomeroy, J. W., & Marsh, P. (2017). Diagnosis of the hydrology of a small Arctic basin at the tundra-taiga transition using a physically based hydrological model. *Journal of Hydrology, 550*, 685-703.

Krogh, S. A., Pomeroy, J. W., & McPhee, J. (2015). Physically based mountain hydrological modeling using reanalysis data in Patagonia. *Journal of Hydrometeorology, 16*(1), 172-193.

Kurylyk, B. L., Hayashi, M., Quinton, W. L., Mackenzie, J. M., & Voss, C. I. (2016). Influence of vertical and lateral heat transfer on permafrost thaw, peatland landscape transition, and groundwater flow. *Water Resources Research, 52*(2), 1286-1305.

Kwong, Y. J., & Gan, T. Y. (1994). Northward migration of permafrost along the Mackenzie Highway and climatic warming. *Climatic Change, 26*(4), 399-419.

Lafleur, P. M., & Roulet, N. T. (1992). A comparison of evaporation rates from two fens of the Hudson Bay Lowland. *Aquatic Botany, 44*(1), 59-69.

Leavesley, G. H., Lichty, R. W., & Troutman, B. S. (1983). *Precipitation-runoff modelling system: user's manual. Report 83-4238.* Washington DC, US: Us Geological Survey Water Resources Investigations.

Lopez-Moreno, J. I., Pomeroy, J. W., Revuelto, J., & Vicente-Serrano, S. M. (2013). Response of snow processes to climate change: spatial variability in a small basin in the Spanish Pyrenees. *Hydrological Processes, 27*(18), 2637-2650.

Luce, C. H., & Tarboton, D. G. (2010). Evaluation of alternative formulae for calculation of surface temperature in snowmelt models using frequency analysis of temperature observations. *Hydrology and Earth System Sciences, 14*(3), 535-543.

Mahmood, T. H., Pomeroy, J. W., Wheater, H. S., & Baulch, H. M. (2017). Hydrological responses to climatic variability in a cold agricultural region. *Hydrological Processes, 31*(4), 854-870.

Marsh, P., Russel, M., Pohl, S., Haywood, H., & Onclin, C. (2009). Changes in thaw lake drainage in the Western Canadian Arctic from 1950 to 2000. *Hydrological Processes, 23*(1), 145-158.

McClymont, A. F., Hayashi, M., Bentley, L. R., & Christensen, B. S. (2013). Geophysical imaging and thermal modeling of subsurface morphology and thaw evolution of discontinuous permafrost. *Journal of Geophysical Research: Earth Syrface, 118*(3), 1826-1837.

Mohammed, A. A., Schincariol, R. A., Quinton, W. L., Nagare, R. M., & Flerchinger, G. N. (2017). On the use of mulching to mitigate permafrost thaw due to linear disturbances in sub-arctic peatlands. *Ecological Engineering, 102*, 207-223.

Monteith, J. L. (1965). Evaporation and environment. *19th Symposium of the Society for Experimental Biology* (pp. 205-234). Cambridge: Cambridge University Press.

Nichols, D. S., & Brown, J. M. (1980). Evaporation from a sphagnum moss surface. *Journal of Hydrology, 48*(3-4), 289-302.

O'Donnell, J. A., Jorgenson, M. T., Harden, J. W., McGuire, A. D., Kanevskiy, M. Z., & Wickland, K. P. (2012). The effects of permafrost thaw on soil hydrologic, thermal, and carbon dynamics in an Alaskan peatland. *Ecosystems, 15*(2), 213-229.

O'Donnell, J. A., Romanovsky, V. E., Harden, J. W., & McGuire, A. D. (2009). The effect of moisture content on the thermal conductivity of moss and organic soil horizons from black spruce ecosystems in interior Alaska. *Soil Science, 174*(12), 646-651.

Pan, X., Yang, D., Li, Y., Barr, A., Helgason, W., Hayashi, M., . . . Janowicz, R. J. (2016). Bias corrections of precipitation measurements across experimental sites in different ecoclimatic regions of western Canada. *The Cryosphere, 10*(5), 2347-2360.

Patankar, R., Quinton, W. L., Hayashi, M., & Baltzer, J. L. (2015). Sap flow responses to seasonal thaw and permafrost degradation in a subarctic boreal peatland. *Trees, 29*(1), 129-142.

Pelletier, N., Talbot, J., Olefeldt, D., Turetsky, M., Blodau, C., Sonnentag, O., & Quinton, W. L. (2017). Influence of Holocene permafrost aggradation and thaw on the paleoecology and

carbon storage of a peatland complex in northwestern Canada. *The Holocene, 27*(9), 1391-1405.

Pietroniro, A., Prowse, T., Hamlin, L., Kouwen, N., & Soulis, R. (1996). Application of a grouped response unit hydrological model to a northern wetland region. *Hydrological Processes, 10*(10), 1245-1261.

Pomeroy, J. W., & Li, L. (2000). Prairie and arctic areal snow cover mass balance using a blowing snow model. *Journal of Geophysical Research: Atmospheres, 105*(D21), 26619-26634.

Pomeroy, J. W., Fang, X., & Marks, D. G. (2016). The cold rain-on-snow event of June 2013 in the Canadian Rockies - characteristics and diagnoses. *Hydrological Processes, 30*(17), 2899-2914.

Pomeroy, J. W., Gray, D. M., Brown, T., Hedstrom, N. R., Quinton, W. L., Granger, R. J., & Carey, S. K. (2007). The cold regions hydrological model: a platform for basing process representation and model structure on physical evidence. *Hydrological Processes, 21*(19), 2650-2667.

Pomeroy, J., Fang, X., & Ellis, C. (2012). Sensitivity of snowmelt hydrology in Marmot Creek, Alberta, to forest cover disturbance. *Hydrological Processes, 26*(12), 1891-1904.

Price, J. S. (1987). The influence of wetland and mineral terrain. *Canadian Water Resources Journal, 12*(2), 43-52.

Price, J. S., & Fitzgibbon, J. E. (1987). Groundwater storage-streamflow relations during winter in a subarctic wetland, Saskatchewan. *Canadian Journal of Earth Sciences, 24*(10), 2074-2081.

Priestley, C. H., & Taylor, R. J. (1972). On the assessment of surface heat flux and evaporation using large-scale parameters. *Monthly Weather Review, 100*(2), 81-92.

Quinton, W. L., & Baltzer, J. L. (2013). The active-layer hydrology of a peat plateau with thawing permafrost (scotty Creek, Canada). *Hydrogeology Journal, 21*(1), 201-220.

Quinton, W. L., & Hayashi, M. (2005). The flow and storage of water in the wetland-dominated central Mackenzie river basin: Recent advances and future directions. In *Prediction in Ungauged Basins: Approaches for Canada's Cold Regions* (pp. 45-56). Cambridge: Canadian Water Resources Association.

Quinton, W. L., & Hayashi, M. (2008). Recent advances towards physically-based runoff modeling of the wetland-dominated central Mackenzie River Basin. In M. K. Woo, W. R. Rouse, R. E. Stewart, & J. M. Stone, *Cold Region Atmospheric and Hydrologic Studies: The Mackenzie GEWEX experience* (pp. 257-279). Springer Berlin Heidelberg.

Quinton, W. L., Hayashi, M., & Carey, S. K. (2008). Peat hydraulic conductivity in cold regions and its relation to pore size and geometry. *Hydrological Processes, 22*, 2829-2837.

Quinton, W. L., Hayashi, M., & Chasmer, L. E. (2009). Peatland hydrology of discontinuous permafrost in the Northwest Territories: overview and synthesis. *Canadian Water Resources Journal, 34*(4), 311-328.

Quinton, W. L., Hayashi, M., & Chasmer, L. E. (2011). Permafrost-thaw induced land-cover change in the Canadian subarctic: implications for water resources. *Hydrological Processes, 25*(1), 152-158.

Quinton, W. L., Hayashi, M., & Pietroniro, A. (2003). Connectivity and storage functions of channel fens and flat bogs in northern basins. *Hydrological Processes, 17*(18), 3665-3684.

R Core Team. (2017). R: A language and environment for statistical computing. Vienna, Austria: R Foundation for Statistical Computing. Retrieved from https://www.R-project.org/

Rasouli, K., Pomeroy, J. W., Janowicz, J. R., Carey, S. K., & Williams, T. J. (2014). Hydrological sensitivity of a northern mountain basin to climate change. *Hydrological Processes, 28*(14), 4191-4208.

Roulet, N. T., & Woo, M. K. (1986). Hydrology of a wetland in the continuous permafrost region. *Journal of Hydrology, 89*(1-2), 73-91.

Shook, K. (2016). CRHMr: Pre- and post-processing for CRHM. *R package version 2.4.10*. Retrieved from https://github.com/CentreForHydrology/CRHMr

Sicart, J. E., Pomeroy, J. W., Essery, R. L., & Bewley, D. (2006). Incoming longwave radiation to melting snow: observations, sensitivity and estimation in northern environments. *Hydrological Processes, 20*(17), 3697-3708.

Sjöberg, Y., Coon, E., Sannel, K., Britta, A., Pannetier, R., Harp, D., . . . Lyon, S. W. (2016). Thermal effects of groundwater flow through subarctic fens; A case study based on field observations and numerical modeling. *Water Resources Research, 52*, 1591-1606.

Smith, C. D. (2007). Correcting the wind bias in snowfall measurements made with a Geonor T-200B precipitation gauge and alter wind shield. *87th American Meteorological Socitey Meeting*, *36*, pp. 162-167. San Antonio, Texas.

Smith, S. L., M. M. Burgess, D. R., & Nixon, M. F. (2005). Recent trends from Canadian permafrost thermal monitoring network sites. *Permafrost and Periglacial Processes, 16*(1), 19-30.

Spence, C., & Woo, M. K. (2006). Hydrology of subarctic Canadian Shield: heterogeneous headwater basins. *Journal of Hydrology, 317*(1), 138-154.

St Jacques, J. M., & Sauchyn, D. J. (2009). Increasing winter baseflow and mean annual streamflow from possible permafrost thawing in the Northwest Territories, Canada. *Geophysical Research Letters, 36*(1).

Tarnocai, C. (2006). The effect of climate change on carbon in Canadian peatlands. *Global and planetary Change, 53*(4), 222-232.

Taylor, A. E., Wang, K., Smith, S. L., Burgess, M. M., & Judge, A. S. (2006). Canadian Arctic Permafrost Observatories: Detecting contemporary climate change through inversion of subsurface temperature time series. *Journal of Geophysical Research: Solid Earth, 111*.

Verseghy, D. L. (1991). CLASS - A Canadian land surface scheme for GCMs. I. Soil model. *Interbational Journal of Climatology, 11*(2), 111-133.

Vickers, D., & Mahrt, L. (1997). Quality control and flux sampling problems for tower and aircraft data. *Journal of Atmospheric and Oceanic Technology, 14*, 512-526.

Warren, R. K., Pappas, C., Helbig, M., Chasmer, L. E., Berg, A. A., Baltzer, J. L., . . . Sonnentag, O. (in review). Minor contributions of overstory transpiration to landscape evapotranspiration in boreal permafrost peatlands. *Ecohydrology*.

Weber, M., Bernhardt, M., Pomeory, J. W., Fang, X., Harer, S., & Schultz, K. (2016). Description of current and future snow processes in a small basin in the Bavarian Alps. *Environmental Earth Sciences, 75*(17), 1-18.

Whittington, P. N., & Price, J. S. (2006). The effects of water table draw-down (as a surrogate for climate change) on the hydrology of a fen peatland. *Hydrological Processes, 20*(17), 3589-3600.

Williams, T. J., Pomeroy, J. W., Janowicz, J. R., Carey, S. K., Rasouli, K., & Quinton, W. L. (2015). A radiative-conductive-convective approach to calculate thaw season ground surface temperatures for modelling frost table dynamics. *Hydrological Processes, 29*(18), 3945-3965.

Williams, T. J., Quinton, W. L., & Baltzer, J. L. (2013). Linear disturbances on discontinuous permafrost: implications for thaw-induced changes to land cover and drainage patterns. *Environmental Research Letters, 8*(2), 025006.

Woo, M. K., & Winter, T. C. (1993). The role of permafrost and seasonal frost in the hydrology of northern wetlands in North America. *Journal of Hydrology, 141*(1-4), 5-31.

Wright, N., Quniton, W. L., & Hayashi, M. (2008). Hillslope runoff from an ice-cored peat plateau in a discontinuous permafrost basin, Northwest Territories, Canada. *Hydrological Processes, 22*(15), 2816-2828.

Zambrano-Bigiarini, M. (2014). hydroGOF: Goodness-of-fit functions for comparison of simulated nad observed hydrological time series. *R package version 0.3-8*. Retrieved from https://CRAN.R-project.org/package=hydroGOF

Zha, T., Barr, A. G., van der Kamp, G., Black, T. A., McCaughey, J. H., & Flanagan, L. B. (2010). Interannual variation of evapotranspiration from forest and grassland ecosystems in westn Canada in relation to drought. *Agrciultural and Forest Meteorology, 150*(11), 1476-1484.

Zhang, Y., Carey, S. K., Quinton, W. L., Janowicz, J. R., Pomeroy, J. W., & Flerchinger, G. N. (2010). Comparison of algorithms and parameterisations for infiltration into organic-covered permafrost soils. *Hydrology and Earth System Scienes, 14*(5), 729-750.

Zhao, L., & Gray, D. M. (1999). Estimating snowmelt infiltration into frozen soils. *Hydrological Processes, 13*(12), 1827-1842.

Zhou, J., Pomeroy, J. W., Zhang, W., Cheng, G., Wang, G., & Chen, C. (2014). Simulating cold regions hydrological processes using a modular model in the west of China. *Journal of Hydrology, 509*, 13-24.

5. SUPPLEMENTAL MATERIALS

5.1 Details on Water Balance

Surface discharge was calculated as a flux between two water level recorders using Manning's formula,

$$Qsur = \frac{1}{n} A R_h^{\frac{2}{3}} S^{\frac{1}{2}}, \text{ where for } w \gg d, R_h = d \quad (3)$$

The cross sectional area, A [m^2], is the width of the fen multiplied by the depth of water above the surface at the location of the upstream water level recorder. The hydraulic radius, Rh [m], was approximated using the depth of water above the surface of the upstream water level recorder, as the fen width is significantly larger than the water depth. The slope of the water surface between the upstream and downstream water level recorder was calculated using DGPS elevation of the underlying wetland surface and adding the height of the water table above the fen surface, and dividing by the straight line distance between the water level recorders. Manning's roughness coefficient, n [s/m$^{1/3}$], was calculated by rearranging Manning's equation and using a velocity derived from the measured celerity, c [m/s], in response to a large summer rain event.

$$n = d^{\frac{2}{3}} S^{\frac{1}{2}} \frac{5}{3c} \quad (4)$$

Average discharge rates for each 30-minute interval were summed to obtain total daily surface discharge. The daily discharge was then divided by the surface area of the fen which was derived from a land cover classification map of the basin (Chasmer et al., 2014) to obtain the daily flux, *Qsur* [mm/day].

Subsurface discharge was calculated only for the saturated layer below the water table using Darcy's Law,

$$Qsub = kA \frac{h_1 - h_2}{L} \quad (5)$$

where the area, A [m^2], is the width of the fen multiplied by the depth of saturated peat at the location of the downstream water level recorder. The depth of saturated peat is the distance between the full depth of the peat profile, as determined by field sampling, and the top of the saturated layer as recorded by the water level recorder. The hydraulic head, h [m], was determined using the DGPS measured elevation at the location of the water level recorder added to the depth of water relative to the surface. The distance between water level recorders, L [m], was determined using DGPS location. The saturated hydraulic conductivity of a channel fen, k [m/s], was determined to have the following relationship with the depth from peat surface from field fen tracer tests conducted in the year 2000, 2003 and 2005 (Hayashi & Quinton, 2005)

$$k = 0.7701e^{3.8342d_p} \quad (6)$$

An average saturated hydraulic conductivity was calculated by taking the integral of the above relationship over the depth of saturated peat. The average half hourly discharge was summed to a daily flux, *Qsub* [mm/day], using the same method as that of surface discharge.

5.2 Details on CRHM Modules

The modules outlined in Figure 11 chosen to represent the processes in this sub-basin are as follows (module name and variation number in brackets):

1. Observations (obs): makes input meteorological data (wind speed, temperature, relative humidity, incoming shortwave radiation, precipitation) available to other modules.
2. Sunshine Hour (calcsun#1): uses incoming shortwave radiation to estimate sunshine hours; used as input to net all-wave radiation and snowmelt modules.
3. Longwave Radiation (longVt): uses incoming shortwave radiation to calculate incoming longwave radiation; used as input to canopy module (Sicart et al., 2006).

4. Net Radiation (netall): calculates the snow-free net all-wave radiation from the estimated shortwave radiation (Garnier & Ohmura, 1970) and the estimated net longwave radiation (Brunt, 1932) using air temperature, vapor pressure, and actual sunshine hours (Granger & Gray, 1990); used as input to evapotranspiration and ground surface temperature modules.
5. Evapotranspiration (evap_Resist): uses Priestley-Taylor evaporation equations (Priestley & Taylor, 1972) to calculate evaporation from saturated surfaces (wetlands and lake) and uses Penman-Monteith evaporation equations (Monteith, 1965) to calculate actual evaporation from the soil column in HRUs with unsaturated surfaces (peat plateau).
6. Canopy(CanopyClearingGap#1): estimates the sub-canopy shortwave and longwave radiation and canopy interception of snowfall and rainfall, and updates under-canopy snowfall and rainfall. The module has options for a full forest canopy, a forest clearing gap, or a completely open area with no canopy effects (Ellis et al., 2010).
7. Snow Albedo (albedo_Richard): calculates snow albedo during winter and melt periods (Verseghy, 1991), used as input to energy-budget snowmelt module.
8. Blowing Snow (pbsm): simulates snow sublimation and transport between HRUs based on surface aerodynamic roughness (Pomeroy & Li, 2000).
9. Energy-Budget Snowmelt (ebsm#1): calculates snowmelt for snowpack using energy balance of net radiation, sensible and latent heat, and advection from rainfall, and change in internal energy (Gray & Landine, 1988).
10. Infiltration (frozenAyers): calculates snowmelt infiltration into frozen soils using Gray's snowmelt infiltration algorithm (Zhao & Gray, 1999) and rainfall infiltration into unfrozen soils based on soil texture and ground cover (Ayers, 1959).

11. Ground Surface Temperature (tsurface#3): calculates the ground surface temperature using air temperature and thermal conductivity and energy of snowpack during snowcover period based on conduction approach (Luce & Tarboton, 2010) and using air temperature and net radiation for snow-free period based on radiative-conductive-convective approach (Williams et al., 2015).
12. Freeze and Thaw Soil Layers (XG): a freeze-thaw algorithm using a simplified solution of Stefan's heat flow equation (Changwei & Gough, 2013) for user defined number of soil layers. Uses ground surface temperature as input.
13. Hydraulic Conductivity (K_Estimate): estimates drainage factors based on Darcy's law for unsaturated hydraulic conductivity using the Brooks and Corey relationship (Fang et al., 2013). Provides the drainage factors for soil moisture balance module.
14. Soil Moisture Balance (SoilX): estimates soil moisture, groundwater flow, and interactions between groundwater and surface water (Leavesley et al., 1983; Fang et al., 2010). Interacts with XG module to account for permafrost.
15. Muskingum Distributed Routing (Netroute_M_D): routes runoff between HRUs and to the sub-basin outlet using Muskingum method (Chow, 1964). The routing does not have to be linear; one HRU can contribute to multiple HRUs (Fang et al., 2010).

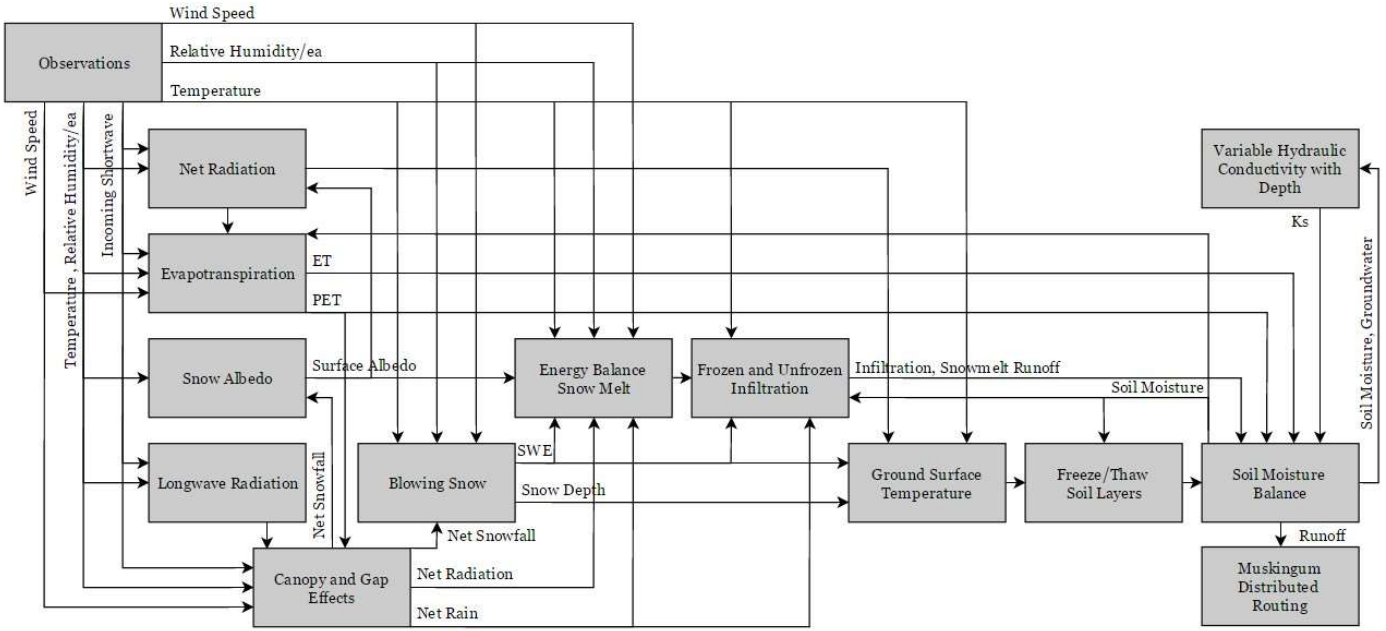

Figure 11. Cold Regions Hydrological Modelling platform (CRHM) modules used to model physical processes of the sub-arctic muskeg. Lines indicate workflow.

5.3 CRHM Module Parameters and Sources

Module	Parameter Name	HRU 1	HRU 2	HRU 3	HRU 4	Source
Shared	basin_area	0.4496				ArcMap 10.4 spatial analysis of 2010 LiDAR DEM
	gw_K	0	0	0	0	
	hru_area	0.2	0.05215	0.08488	0.1126	ArcMap 10.4 spatial analysis of 2010 LiDAR DEM, (Chasmer et al., 2011) land classification
	hru_ASL	0	90	0	0	ArcMap 10.4 spatial analysis of 2010 LiDAR DEM
	hru_elev	269.5	270.9	270.5	271.4	ArcMap 10.4 spatial analysis of 2010 LiDAR DEM
	gru_GSL	0.0262	0.03	0.15	2.09	ArcMap 10.4 spatial analysis of 2010 LiDAR DEM
	hru_lat	61.3	61.3	61.3	61.3	ArcMap 10.4 spatial analysis of 2010 LiDAR DEM
	Ht	0.001	0.05	0.1	3.1	(Wright et al., 2008)
	inhibit_evap	0	0	0	0	
	lower_ssr_K	0	0	0	0	
	rechr_ssr_K	0	0	0	0	

	Sdmax	1000	150	280	0	Lake: estimated lake depth, Bog: Max level of water in old camp bog water table, Fen: Average maximum reading of fen WLRs in 2015
	Sd_gw_K	0	0	0	0	
	Sd_ssr_K	0	0	0	0	
	Si	0	0.6	0.6	0.5	
	soil_Depth	0	0.25	0.25	0.7	Modeled soil depth above groundwater layer. For Bogs and Fens modeled maximum evap depth plus 5cm buffer. Max evap depth in northern sphagnum peatland is 20cm (Nichols & Brown 1980; Kim & Verma 1996). In plateau model depth to permafrost table.
	soil_gw_K	0	0	0	0	
	soil_moist_max	0	213	213	408	depth of modelled soil layer * porosity
	soil_rechr_max	0	173	173	133	depth of modelled upper soil layer in which ET occurs * porosity
	soil_type	10	10	10	10	
	Zwind	2	2	2	2.1	installation height of measured wind speed
albedo_Richard	a1	1.08E+07	1.08E+07	1.08E+07	1.08E+07	
	a2	7.20E+05	7.20E+05	7.20E+05	7.20E+05	

	Albedo_Bare	0.1	0.17	0.17	0.137	Bog/Fen albedo calculated from measured SW in/out between June 1st and Sept 30 from input bog tripod data. Plateau same dates measured SW in/out from plateau tripod.
	Albedo_Snow	0.85	0.85	0.85	0.85	
	amax	0.84	0.84	0.84	0.82	
	amin	0.5	0.5	0.5	0.5	
	smin	1	1	1	3	
basin	basin_name	FenWatershed				
	hru_names	Lake	Bog	Fen	Plateau	
	INIT_STATE					
	Loop_to					
	RapidAdvance_to					
	RUN_END	0				
	RUN_ID	1				
	RUN_START	0				
	StaeVars_to_Update					
	TraceVars					
CanopyClearingGap	Alpha_c	0.1	0.1	0.1	0.1	
	B_canopy	0.038	0.038	0.038	0.038	
	CanopyClearing	1	2	1	0	
	Gap_diameter	565	41	150	100	ArcMap 10.4 spatial analysis of 2010 LiDAR DEM
	LAI	0	0	0	0.9	(Baltzer et al., 2014).
	sBar	0	0	0.5	3.3	
	Surrounding_Ht	3.1	3.1	3.1	3.1	(Wright et al., 2008)

	unload_t	1	1	1	-3	
	unload_t_water	6	4	6	6	
	Z0snow	0.01	0.01	0.01	0.01	
	Zref	1.9	1.9	1.9	2.15	Bog and Plateau tripod instrument heights measured when installed.
	Zvent	0.75	0.75	0.75	0.75	
ebsm	daily_melt	0	0	0	0	
	Qe_subl_from_SWE	0	0	0	0	
evap_Resist	evap_type	2	2	2	0	
	F_Qg	0.75	0.3	0.3	0.2	(Hayashi et al., 2007)
	Htmax	0.1	0.1	0.5	3.1	(Wright et al., 2008)
	LAImax	0.1	0.1	0.2	0.9	(Baltzer et al., 2014).
	LAImin	0.1	0.1	0.2	0.9	(Baltzer et al., 2014).
	Pmmethod	1	1	1	1	
	rcs	25	200	200	223	(Kellner, 2001; Zha et al., 2010)
	s	1	0	1	1	
frozenAyers	C	1	1	1	1	
	groundcover	1	3	5	6	
	hru_tsoil	269.1	269.1	269.1	269.1	(Quinton & Hayashi, 2008)
	S0	1	0.8	0.8	0.8	(Quinton & Hayashi, 2008)
	t0	0	0	0	0	
	t0_julian	0				
	texture	1	1	1	1	
	t_ice_lens	-20	-20	-20	-20	
global	Time_Offset	1.09	1.09	1.09	1.09	(Cornwall et al., 2015)
K_estimate	Inhibit_K_set	0	0	0	0	

	Ks_gw	1.74E-07	2.11E-08	2.11E-08	1.74E-05	(Christensen 2014)
	Ks_lower	3.68E-05	7.57E-08	7.57E-08	1.74E-05	(Christensen 2014; Quinton et al., 2008)
	Ks_upper	0.002683	0.000121	0.000121	0.003606	(Quinton et al., 2008)
	PSD	5.6	5.6	5.6	5.6	(Zhang et al., 2010)
longVT	epsilon_s	0.98	0.98	0.98	0.98	
	Vt	0	0	0	0	
Netroute_M_D	Channel_sho	0	0	0	0	
	distrib_Basin	0	0	1	0	
	distrib_Route[1]	0	0	1	0	(Fang et al., 2010)
	distrib_Route[2]	0	0	1	0	(Fang et al., 2010)
	distrib_Route[3]	0	0	0	0	(Fang et al., 2010)
	distrib_Route[4]	0	0.4194	0.5806	0	(Fang et al., 2010)
	gwKstorage	20	5	20	0	
	gwLag	0	0	0	0	
	gwwhereto	-3	-3	0	-2	(Quinton et al., 2009)
	Lag	0	0	0	0	
	order	1	3	4	2	
	route_L	250	27	313.5	37.5	ArcMap 10.4 spatial analysis of 2010 LiDAR DEM
	route_n	0.016	0.03	0.07	0.2	(Chow, 1959)
	route_R	0.5	0.075	0.25	0.03	Water level recorder data
	route_S0	0.000457	0.000524	0.002618	0.03649	ArcMap 10.4 spatial analysis of 2010 LiDAR DEM
	route_X_M	0.25	0.25	0.25	0.25	
	runKstorage	0	0.0014	1	0.0028	
	runLag	0	0	0	0	
	scaling_factor	1	1	1	1	

	Sd_ByPass	0	0	0	0	
	soil_rechr_ByPass	0	0	0	0	
	ssrKstorage	1.1	2.6	30	0.12	
	ssrLag	0	0	0	0	
obs	catchadjust	0	0	0	0	
	ClimChng_flag	0	0	0	0	
	ClimChng_precip	1	1	1	1	
	ClimChng_t	0	0	0	0	
	ElevChng_flag	0	0	0	0	
	HRU_OBS[1]	2	2	2	1	
	HRU_OBS[2]	1	1	1	1	
	HRU_OBS[3]	2	2	2	1	
	HRU_OBS[4]	2	2	2	1	
	HRU_OBS[5]	2	2	2	1	
	lapse_rate	0.75	0.75	0.75	0.75	
	obs_elev	269.7	270.9	270.5	271.4	ArcMap 10.4 spatial analysis of 2010 LiDAR DEM
	ppt_daily_distrib	1	1	1	1	
	precip_elev_adj	0	0	0	0	
	snow_rain_determination	2	2	2	2	
	tmax_allrain	4	4	4	4	
	tmax_allsnow	0	0	0	0	
pbsm	A_S	0	0.003	0.003	0.1	
	distrib	1	1	3	10	
	fetch	300	300	300	300	
	inhibit_bs	0	0	0	0	
	inhibit_subl	0	0	0	0	
	N_S	1	75	75	1	(Wright et al., 2008)

SoilX	cov_type	2	2	2	2	
	Dts_organic_init	0	0	0	0	
	Dts_organic_max	0	0	0	0	
	Dts_organic_runoff_K	0	0	0	0	
	Dts_snow_init	0	0	0	0	
	Dts_snow_max	0	0	0	0	
	Dts_snow_runoff_K	0	0	0	0	
	evap_from_runoff	1	1	1	1	
	gw_init	1596	1554	1554	0	Depth between mineral layer and modeled upper soil layer (4.0m-0.25m=3.75m) * lower porosity. No groundwater under modeled soil layer for Plateau because it's permafrost/frozen.
	gw_max	1596	1554	1554	0	
	NO_Freeze	1	1	1	0	
	porosity_lower	0.42	0.8	0.8	0.55	(Quinton et al., 2008; Zhang et al., 2010)
	porosity_upper	0.53	0.865	0.865	0.665	(Quinton et al., 2008; Zhang et al., 2010)
	Sdinit	900	0	0	0	
	soil_moist_init	0	127.8	127.8	204	
	soil_rechr_init	0	103.8	103.8	66.5	
	soil_ssr_runoff	0	1	1	1	
	soil_withdrawal	2	1	1	4	
	transp_limited	0	1	1	0	
tsurface	W_a	0.77	0.77	0.77	0.77	
	W_b	0.02	0.02	0.02	0.02	

	W_c	7	7	7	7	
	W_d	0.03	0.03	0.03	0.03	
Volumetric	fallstat	0	0	0	0	
	set_fallstat	305	305	305	305	
	Si_correction	0	0	0	0	
XG	calc_conductivity	1	1	1	1	
	depths[1:4]	0.05	0.05	0.05	0.05	
	depths[5:18]	0.1	0.1	0.1	0.1	
	freeze_kw_ki_update	1	1	1	1	
	k_update	2	2	2	2	
	N_Soil_layers	18	18	18	18	
	por[1:5]	0.53	0.865	0.865	0.665	(Quinton et al., 2008; Zhang et al., 2010)
	por[5:18]	0.42	0.8	0.8	0.55	(Quinton et al., 2008; Zhang et al., 2010)
	soil_solid_km[1:18]	0.05	0.05	0.05	0.05	(O'Donnell et al., 2009)
	soil_solid_ki[1:18]	1.9	1.9	1.9	1.9	(Woo 2012)
	soil_soild_kw[1:18]	0.58	0.58	0.58	0.58	(O'Donnell et al., 2009)
	SWE_k	0.35	0.35	0.35	0.35	
	thaw_ki_kw_update	1	1	1	1	
	theta_default[1:4]	1	0.2	0.2	0.2	(Quinton et al., 2005)
	theta_default[5:7]	1	1	1	0.2	(Quinton et al., 2005)
	theta_default[8:18]	1	1	1	0.7	(Quinton et al., 2005)
	theta_min	0.1	0.1	0.1	0.1	(Quinton et al., 2005)
	Trigthrhld	100	100	100	100	
	Zdf_init	0	0	0	0	
	Zdt_init	2	3	3	2	
	Zpf_init	2	3	3	2	